

ATTACHMENT A



FINAL REPORT

**DETERMINISTIC EARTHQUAKE
GROUND MOTIONS ANALYSIS**

**PRIVATE FUEL STORAGE FACILITY
SKULL VALLEY, UTAH**

Prepared for:

**Stone & Webster Engineering Corporation
CS-028233 J.O. NO. 0599601-005**

Prepared by:

**Geomatrix Consultants, Inc.
and
William Lettis & Associates, Inc.**

March 1997

GMX #3801.1 (REV. 0)

9907160167 990709
PDR ADOCK 07200022
C PDR

Geomatrix Consultants



SWEC #0599601-005
GMX #3801-1 (REV. 0)

DETERMINISTIC EARTHQUAKE GROUND MOTIONS ANALYSIS
PRIVATE FUEL STORAGE FACILITY, SKULL VALLEY, UTAH

Prepared for:

Stone & Webster Engineering Corporation

Prepared by: Robert R. Youngs Date: 3/10/97
Reviewed by: Kathryn L. Hanson Date: 3/10/97
Approved by: Kevin J. Coppersmith Date: 3/10/97

QA Category I

Geomatrix Consultants, Inc.
San Francisco, CA

TABLE OF CONTENTS

	PAGE
1.0 INTRODUCTION	1
2.0 SEISMOTECTONIC SETTING.....	3
2.1 Seismotectonic Provinces.....	3
2.2 Tensile Stresses and Active Crustal Extension in the Site Region.....	5
3.0 REGIONAL POTENTIAL SEISMOGENIC SOURCES	9
3.1 Potential Fault Sources Between 100 and 320 km of the Skull Valley Site	9
3.2 Potential Fault Sources Within 100 km of the Skull Valley Site	11
3.2.1 Stansbury Fault	11
3.2.2 East Cedar Mountains Fault.....	13
3.2.3 West Cedar Mountains Fault	15
3.2.4 Clover Fault Zone	15
3.2.5 Mid-Valley Horst Faults	16
3.2.6 Lookout Pass Fault.....	17
3.2.7 Mercur-Topliff Hill Fault Zone	17
3.2.8 Sheeprock Fault Zone	19
3.2.9 Oquirrh Fault Zone	19
3.2.10 Vernon Hills Fault Zone	20
3.2.11 Lakeside Mountains Fault.....	21
3.2.12 Simpson Mountains Fault	21
3.2.13 Sheeprock Mountains Fault	21
3.2.14 Puddle Valley Fault Zone	22
3.2.15 East Great Salt Lake Fault Zone	22
3.2.16 East Tintic Mountains Fault.....	23
3.2.17 West Valley Fault Zone	23
3.2.18 East Lakeside Mountains Fault Zone.....	24
3.2.19 Utah Lake Fault Zone	24
3.2.20 Drum Mountains Fault Zone.....	25
3.2.21 Fish Springs Fault	25
3.2.22 Wasatch Fault Zone	26
3.2.23 West Deep Creek Fault.....	27
3.3 Other Mapped Features in the Vicinity of the Skull Valley Site.....	27
3.3.1 Hickman Knolls Fault and Lineament Zone.....	27
3.3.2 Northwest Hickman Knolls Lineament Zone	29
3.3.3 Springline Fault.....	30
3.3.4 Faults Identified by Geosphere Midwest (1997)	30
4.0 DETERMINISTIC GROUND MOTION ASSESSMENT	32
4.1 Maximum Earthquakes.....	32
4.1.1 Approach.....	32

TABLE OF CONTENTS

	PAGE
4.1.2 Maximum Rupture Lengths	33
4.1.3 Maximum Magnitude Assessments	35
4.2 Ground Motion Assessment	36
4.2.1 Approach	36
4.2.2 Ground Motion Attenuation Relationships	37
4.2.3 Recommended Response Spectra	39
5.0 SUMMARY AND CONCLUSIONS	50
REFERENCES.....	53

TABLES

Table 3-1	Potential capable faults within 100 km of PFSF site
Table 4-1	Stansbury 84th-percentile spectra horizontal spectral accelerations (G)

FIGURES

Figure 2-1	Regional seismotectonic provinces, showing major known late Quaternary faults within 320 km of the site.
Figure 4-1	Seismicity cross sections along the Wasatch Front
Figure 4-2	Sections of the Stansbury and East Cedar Mountains faults. East Cedar Mountains fault after Hood and Waddell (1968); Stansbury fault after Helm (1995), Hecker (1993), and Sack (1993). Triangles show section ends.
Figure 4-3	Maximum magnitude distributions for the Stansbury and East Cedar Mountains faults.
Figure 4-4	Comparison of horizontal PGA Attenuation Relationships
Figure 4-5	Comparison of horizontal acceleration response spectra
Figure 4-6	Comparison of 84th-percentile horizontal response spectra for the three nearby seismic sources
Figure 4-7	Stansbury fault 84th-percentile response spectra
Figure 4-8	Recommended envelope 84th-percentile response spectra

PLATES

Plate 1	Map showing Quaternary faults in the PFSF Site Region
---------	---

FINAL REPORT

DETERMINISTIC EARTHQUAKE GROUND MOTIONS ANALYSIS PRIVATE FUEL STORAGE FACILITY SKULL VALLEY, UTAH P.O. NO. CS-028233, J.O. NO. 05996.01

1.0 INTRODUCTION

This report summarizes a deterministic earthquake ground motion analysis conducted for the proposed Private Fuel Storage Facility (PFSF) in Skull Valley, Utah. This study was conducted for Stone & Webster Engineering Corporation under contract P.O. No. CS-028233, J.O. No. 05996.01. This report incorporates and supersedes the preliminary results given in our Phase 1 report entitled: "Phase 1 Results, Geological and Seismic Consulting Services, Site Seismic Evaluation, Private Fuel Storage Facility."

In the Phase 1 Report, four topics were identified that, in our opinion, needed to be addressed to provide a more defensible assessment of deterministic ground motions (section entitled "Finalizing this Assessment"). All four of these topics were addressed prior to our finalization of this analysis: (1) the lineaments north of Hickman Knolls were evaluated by Prof. Donald Currey (University of Utah) and assessed to be related to lacustrine (lake) depositional processes; (2) geotechnical boreholes and seismic reflection profiles were acquired that provide an interpretation of the depth to bedrock; (3) new published attenuation relationships for normal faulting have been incorporated into this assessment, and (4) geophysical studies were conducted to develop an interpretation of the shear-wave velocity structure beneath the site. With the gathering of this additional information, we are able to develop more confident assessments of ground motions.

The purpose of this study is to develop a deterministic ground motion assessment that can be used for the design of the PFSF. The deterministic methodology has considerable precedent for nuclear power plant design. It provides a conservative estimate because it is based on a series of conservative assumptions: the *maximum* earthquake is assumed to occur on all seismic sources; the maximum earthquake is assumed to occur at the *closest approach* of the

source to the site; and the ground motions are evaluated at the *84th percentile* of the ground motion attenuation relationships. The deterministic methodology followed in this study is identical to that followed in the western U.S. for nuclear power plant studies consistent with Appendix A to 10 CFR Part 100. Because the Skull Valley site lies within a tectonic environment characterized by relatively low seismic activity and long recurrence intervals between large earthquakes, the deterministic methodology provides a very conservative estimate of ground motions.

This report consists of the following: Section 2 summarizes the seismotectonic setting. Section 3 presents the regional potential seismogenic sources, Section 4 presents the characterization of seismic sources and the ground motion assessment. Section 5 presents a summary of this analysis and our conclusions.

2.0 SEISMOTECTONIC SETTING

The Skull Valley PFSF site is located in the central part of the western Cordillera of the United States, an approximately 1300-km-wide region of elevated, mountainous topography that extends from central California on the west to the Great Plains on the east. Orogenic activity within the Cordillera dates back to the Paleozoic, and generally reflects a long history of crustal shortening that continued through the late Cretaceous-early Tertiary Laramide orogeny (Oldow and others, 1989). Mid-Tertiary to Quaternary tectonism within the Cordillera, however, is characterized by crustal extension and is distributed over many hundreds of kilometers east of the transcurrent Pacific/North American plate boundary in California.

2.1 Seismotectonic Provinces

Previous workers have subdivided the western Cordillera into distinct provinces based on physiographic characteristics, volcanic activity, the presence and activity of late Cenozoic faults, and patterns of seismicity. Provinces that lie within 320 km of the PFSF site include the Basin and Range province, the Wasatch Frontal Zone province, the Snake River Plain province, and the Colorado Plateau province (Figure 2-1). We discuss each of these provinces below.

The Skull Valley PFSF site is located within the Basin and Range province. The province is an approximately 400 to 800 km wide region of active crustal extension and distributed normal faulting that is bounded on the west by the Sierra Nevada mountain range in eastern California, and bounded on the east by the Wasatch Frontal Zone province in Utah (Figure 2-1). The Basin and Range province is named for the characteristic topography associated with the development of fault-bounded, tilted structural blocks, which define subparallel, north-trending ranges and intervening internally drained basins. Large-scale crustal extension in the Basin and Range province in Utah began approximately 20 to 21 million years ago (Rowley and others, 1978) and continues to the present. Mountain ranges are several tens of kilometers long and locally attain crustal elevations of approximately 3 km. The floors of the adjacent valleys commonly lie at elevations of approximately 1.2 to 1.5 km. Late Cenozoic and Quaternary normal faults in the Basin and Range typically lie along the bases of the ranges and dip beneath the valleys. The Wasatch fault is considered the eastern boundary of the

Basin and Range province. and given its westward dip, the associated seismicity is in the Basin and Range province. The Basin and Range province has been the source of numerous moderate and large magnitude historical earthquakes, including the 1983 Borah Peak earthquake (M_s 7.3) in Idaho; the 1954 Dixie Valley (M 6.9); 1954 Fairview Peak (M 7.3); and 1915 Pleasant Valley (M 7.8) earthquakes in central Nevada (Rogers and others, 1991); and the 1934 Hansel Valley earthquake (M 6.6) near the northern end of the Great Salt Lake in Utah (Smith and Arabasz, 1991). In general, historical and contemporary seismicity is concentrated along the eastern and western margins of the Basin and Range province, with the exception of the Central Nevada Seismic Belt (de Polo and others, 1989).

The Wasatch Frontal Zone province is a transitional zone between the actively extending Basin and Range province and the tectonically quiescent Colorado Plateau province in northern Utah (Figure 2-1; Jacobs Engineering and others, 1988). The western margin of the province lies about 85 km east of the PFSF site. The Wasatch frontal zone is distinguished from the Basin and Range province by a higher level of background seismicity, and generally higher deformation rates. The major active fault along the western margin of this province is the Wasatch fault zone, an approximately 370 km long, west-dipping normal fault system that has been the source of repeated large magnitude Holocene surface-faulting earthquakes (Machette and others, 1991). The Wasatch Frontal Zone province is part of the central and southern reaches of the Intermountain Seismic Belt, a north-trending zone of active seismicity that extends from southern Nevada and northern Arizona to northwestern Montana (Smith and Arabasz, 1991). The Intermountain Seismic Belt is approximately 100 to 200 km wide, has a generally curvilinear trend along its length, and is characterized by moderate to high levels of shallow crustal seismicity (i.e., hypocentral depths of 20 km or less). Analyses of earthquake focal mechanisms show that seismogenic deformation in the Intermountain Seismic Belt accommodates approximately east-west-directed crustal extension (Eddington and others, 1987; Smith and Arabasz, 1991).

The western margin of the Colorado Plateau province lies approximately 150 km east of the PFSF site (Figure 2-1). In contrast to the Basin and Range province, which locally has accommodated 30% to 100% of horizontal crustal extension during Tertiary time (Christiansen and Yeats, 1992; Wernicke, 1992), the Colorado Plateau is a relatively stable crustal block that has undergone negligible deformation (Christiansen and Yeats, 1992). The

Colorado Plateau also is distinguished from the Wasatch Frontal Zone province to the west by very low levels of background seismicity. Most of the historical seismicity in the Colorado Plateau province has occurred near the Uncompahgre uplift (Sullivan and others, 1980), which lies approximately 475 km east-southeast of the PFSF site.

The Snake River Plain province forms the northern boundary of the site region, approximately 250 km north of the PFSF site (Figure 2-1). In contrast to the rugged topography of the Basin and Range and the Wasatch Frontal Zone provinces to the south, the Snake River Plain is an area of low relief. The province is approximately 600 km long, 70 to 100 km wide, and has an arcuate, concave-northward shape (Malde, 1991). Workers have divided the Snake River Plain province into western and eastern parts based on distinctive patterns of sedimentation, faulting, and late Cenozoic volcanism. The eastern Snake River Plain, which passes through the northern part of the PFSF region, is a bimodal volcanic province characterized by extensive rhyolitic volcanic rocks overlain by basaltic lava flows (Malde, 1991). The rhyolite and basalt are interpreted to mark the presence of a thermal plume, or "hot spot", in the mantle that presently is centered beneath Yellowstone National Park in northwestern Wyoming. Seismicity is concentrated along the southern, northern and eastern margins of the Snake River Plain province, although this seismicity may be associated with Basin and Range-type extension rather than processes within the Snake River Plain. Within eastern Idaho and western Wyoming, most seismicity in this province is associated with the northern continuation of the Intermountain Seismic Belt (Smith and Arabasz, 1991).

2.2 Tensile Stresses and Active Crustal Extension in the Site Region

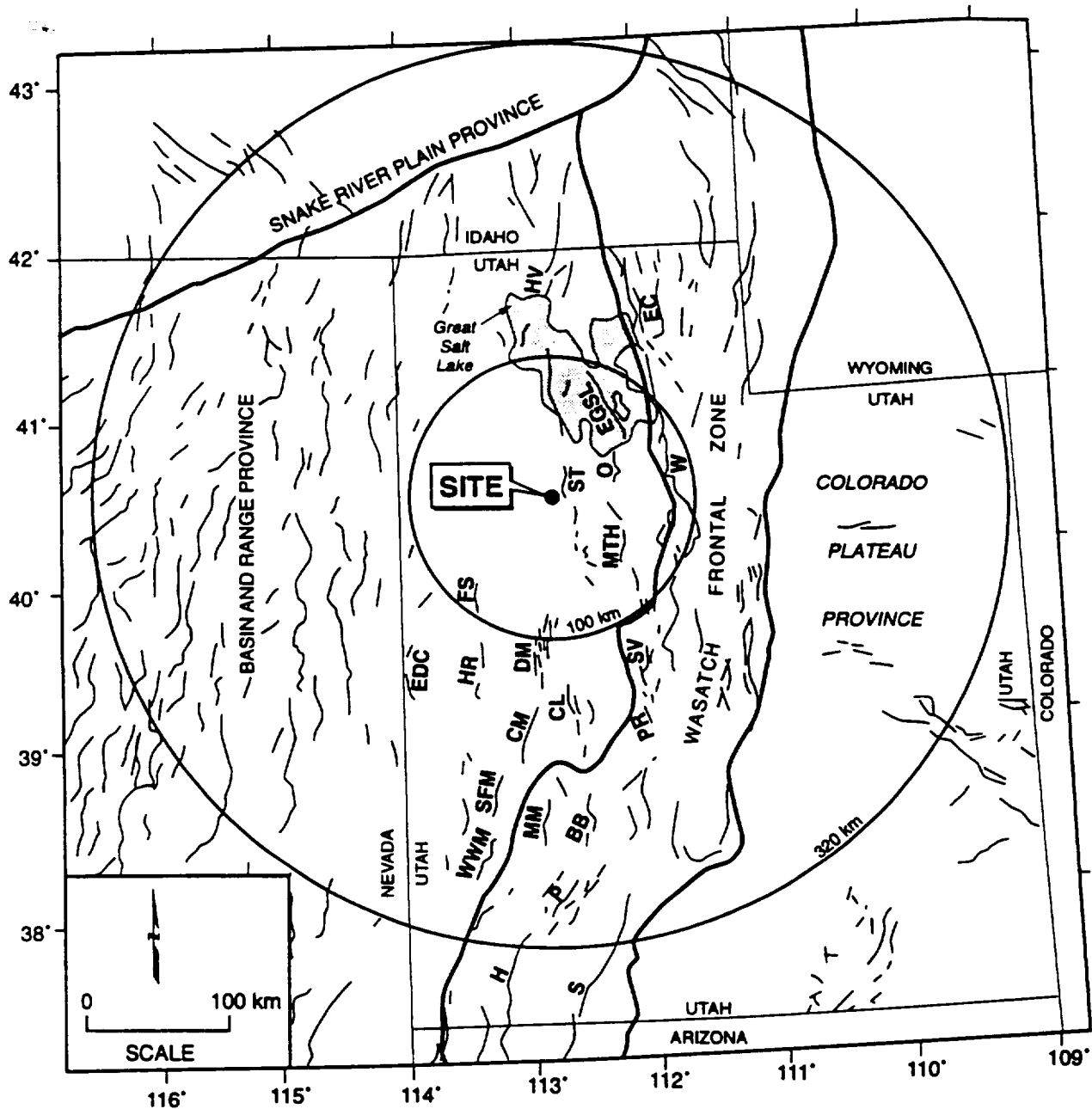
The study region lies within the Cordilleran extensional stress province, which is defined by Zoback and Zoback (1989) to be part of the Rocky Mountain/Intermontane plate-tectonic province. The Cordilleran extensional stress province is approximately 1,700 km wide and is bounded by the Sierra Nevada range in California to the west, and by the Great Plains on the east. Based on earthquake focal mechanisms, the orientation of Quaternary volcanic features, and borehole breakout data, Zoback and Zoback (1989) interpret that the state of stress within this province is characterized by approximately east-west-trending maximum tensile principal stress. The Colorado Plateau also is included in this stress province, although the orientation of the maximum tensile principal stress within the Plateau is inferred to be north-

northeast/south-southwest and thus is anomalous in comparison to regional trends elsewhere in the province (Wong and Humphrey, 1989; Zoback and Zoback, 1989).

The Cordilleran extensional stress province differs from areas of generally compressive horizontal stress to the east and west by its high topography (1.5 to 2.0 km average elevation) and higher average heat flow (Zoback and Zoback, 1989). These characteristic features are significant for assessing the origin of the regional tensile stress and the resulting deformation. Jones and others (1996) propose that the horizontal tensile stress that drives active extension in the western United States arises from gravitational body forces acting on the buoyant, topographically high Cordilleran lithosphere. Simple physical analyses show that variations in the density structure and buoyancy of the lithosphere produce variations in the average lithostatic pressure at depth (Molnar and Lyon-Caen, 1988; England and Jackson, 1989). Because the lithosphere has the mechanical properties of a viscous fluid when viewed at the province scale and over long periods of time (England and Jackson, 1989), the lateral gradients in average lithostatic pressure (also known as the buoyancy force) may cause the lithosphere to flow or spread in order to minimize the pressure differences at depth. The rate of flow for a given magnitude of buoyancy force depends on the average strength of the lithosphere (Jones and others, 1996).

Using models for the tensile strength of the lithosphere, Jones and others (1996) showed that the gravitationally derived buoyancy forces in the Cordilleran extensional stress province are sufficient to drive extension (i.e., "spreading") in the Basin and Range and Wasatch Frontal Zone provinces at a strain rate of approximately $10^{-16} \text{ sec}^{-1}$, which is comparable to the average extension rate in these regions measured by seismologic and geodetic techniques (Eddington and others, 1987; Dixon and others, 1995). For example, the integrated extension rate across the Basin and Range between the Colorado Plateau and the Sierra Nevada is approximately 1 cm/yr, which corresponds to an average strain rate of $10^{-16} \text{ sec}^{-1}$. Because the extension is driven by gravitational forces, the tectonic stresses are present regionally, and thus can be assumed to affect the site area. Areas of the Cordilleran extensional stress province that are not deforming at geologically significant rates, such as the Colorado Plateau and southern Rocky Mountains, represent regions where the lithosphere is stronger and able to support the gravitationally derived tensile forces without significant spreading (Jones and others, 1996). This interpretation suggests that the forces that drive crustal extension in the study region arise

from the local structure and geophysical characteristics of the lithosphere, rather than from the influence of the Pacific/North American plate boundary located more than 1,000 km to the west.



Basin and Range Province Faults

- | | | | |
|------|----------------------|-----|-------------------------|
| CL | Clear Lake | MTH | Mercur-Topliff Hill |
| CM | Cricket Mountains | O | Oquirrh |
| DM | Drum Mountains | SFM | San Francisco Mountains |
| EGSL | East Great Salt Lake | ST | Stansbury |
| FS | Fish Springs | EDC | East Deep Creek |
| HR | House Range | WWM | Wah Wah Mountains |
| HV | Hansel Valley | | |

Wasatch Frontal Zone Faults

- | | |
|----|-------------------|
| BB | Beaver Basin |
| EC | East Cache |
| H | Hurricane |
| MM | Mineral Mountains |
| P | Paragonah |
| PR | Pavant Range |
| S | Sevier |
| SV | Scipio Valley |
| W | Wasatch |

Figure 2-1. Regional seismotectonic provinces, showing major known late Quaternary faults within 320 km of the site.

3.0 REGIONAL POTENTIAL SEISMOGENIC SOURCES

3.1 Potential Fault Sources Between 100 and 320 km of the Skull Valley Site

As noted above, the PFSF site region includes parts of the Basin and Range, Wasatch Frontal Zone, Colorado Plateau and Snake River Plain provinces (Figure 2-1). Each of these provinces contains faults that are potential seismic sources, although at distances of greater than 100 km it is unlikely that any of these potential sources would produce significant ground motions at the PFSF site.

The Basin and Range province contains many normal faults along the margins of north-trending uplifts. In eastern Nevada, many of these faults are potential capable sources, although most have not been previously characterized and none has had historic surface rupture (Rogers and others, 1991). In western Utah, Hecker (1993) shows several north-trending faults that exhibit evidence of late Pleistocene or Holocene activity. These include the East Deep Creek and House Range faults, which are southwest of the PFSF site (Plate 1). The House Range faults are aligned with the Fish Springs fault, which is described below in Section 3.2. South of the PFSF site, a series of north- to northwest-trending faults exhibit evidence of late Quaternary activity. These include the Wah Wah Mountains, San Francisco Mountains, Cricket Mountains, and Drum Mountains faults. The latter of these is within 100 km of the PFSF site and is described in Section 3.2. In northern Utah, Hecker (1993) summarizes the Hansel Valley fault, which experienced surface rupture during the M_w 6.6 Hansel Valley earthquake in 1934 (Doser, 1989). McCalpin and others (1992) suggest that earthquakes comparable in size to the 1934 event may have occurred during times of shallow or no lakes in the Hansel Valley, whereas larger events may have occurred during times when deep lakes occupied the basin. All of the faults in the Basin and Range province between 100 and 320 km from the PFSF site are shorter and(or) probably have lower slip rates than some of the faults within 100 km of the site, and thus are unlikely to produce higher ground motions than nearby sources.

The Wasatch Frontal Zone also contains many faults that exhibit evidence of repeated Holocene and(or) late Pleistocene activity. In northern Utah, this province is dominated by the East Cache and Wasatch fault zones (Plate 1). The East Cache fault zone consists of three

segments, with the central segment exhibiting Holocene movement and the northern and southern segments exhibiting middle to late Pleistocene and late Pleistocene movement, respectively (McCalpin and Forman, 1991). Youngs and others (1987) calculated a maximum earthquake magnitude of 7.25 for the East Cache fault zone. The Wasatch fault is the primary structural feature in central Utah, and consists of nine segments that exhibit either Holocene or late Pleistocene activity (Hecker, 1993). Northeast of the PFSF site, these segments include the Clarkston Mountain, Collingston, Brigham City, and Weber segments (Machette and others, 1992). Hecker (1993) suggests that the Brigham City segment is overdue for a surface-rupturing earthquake on the basis of recurrence intervals and the elapsed time since the most-recent rupture. East of the PFSF site (and within 100 km of the site), the Wasatch fault consists of the Holocene Salt Lake City, Provo, and Nephi segments, which are described below in Section 3.2. Southeast of the PFSF site, the Holocene Levan and late Pleistocene Fayette segments (Machette and others, 1992; Hecker, 1993) are more than 100 km from the PFSF site. The Levan segment is separated from the Nephi segment by a 15-km-long gap in Holocene faulting, and the Fayette segment is less well expressed than other segments of the Wasatch fault.

South of the Wasatch fault, extension in the Wasatch Frontal Zone probably is accommodated by movement on a series of north-trending faults, including the Scipio Valley, Pavant Range, Beaver Basin, Mineral Mountains, and Paragonah faults. These faults exhibit evidence of Holocene or late Pleistocene movement. In the Wasatch Frontal Zone in southern Utah, major faults include the Hurricane and Sevier faults, both of which have had late Pleistocene movement with recurrence intervals of about 5,000 years for earthquakes of M7 or greater, and have slip rates of 0.3 to 0.5 mm/yr (Hecker, 1993).

Based on the fault compilation by Hecker (1993), the Colorado Plateau province within 320 km of the PFSF site contains no faults that exhibit prominent evidence of Holocene or late Pleistocene displacement related to tectonic activity. There are a few west- to northwest-trending faults that exhibit evidence of Quaternary movement, although these are associated with salt dissolution within the Paradox Basin and are more than 250 km from the site. Considering the distances from the PFSF site to the Colorado Plateau or Snake River Plain provinces, it is unlikely that strong ground motions from a source within either of these provinces would be significant at the site. Based on the number of faults having Holocene or

late Pleistocene activity in the Basin and Range and Wasatch Frontal Zone provinces, it is likely that ground motion hazards would be dominated by sources within either of these latter provinces.

3.2 Potential Fault Sources Within 100 km of the Skull Valley Site

Capable and potentially capable sources within 100 km of the PFSF site are listed in Table 3-1, and are discussed below. Plate 1 also shows the location and activity of these potential sources.

3.2.1 Stansbury Fault

The north-trending Stansbury fault forms the border between the western margin of the Stansbury Mountains and the eastern margin of Skull Valley (Plate 1). At its closest location, the fault is 9.5 km from the PFSF site. The Stansbury fault dips to the west, and has had down-to-the-west displacement of late Quaternary alluvium derived from the Stansbury Mountains. Previous investigations show that the fault has had late Quaternary displacement along approximately 40 to 45 km (Hecker, 1993; Helm, 1995). The Stansbury fault as defined by previous workers extends from the northern end of the Stansbury Mountains at the village of Timpie, to Johnson Pass near the village of Willow Springs. Helm (1995) notes that the fault consists of two distinct sections, separated by a west-trending cross fault coincident with Pass Canyon and the southern margin of Salt Mountain. The 20-km-long section of the fault north of Pass Canyon consists of several strands and has a complex pattern of synthetic and antithetic faults. Helm (1995) notes that displacement along the northern section of the fault is partitioned among several strands. The 25-km-long southern section of the fault, in contrast, is comparatively simple, with most of the displacement occurring on a single, distinct strand. Helm (1995) shows that these two sections also are associated with differences in range-crest elevation, plan-view geometry, scarp heights, and drainage-basin asymmetry. In addition, regional gravity data suggests that the basin-fill deposits in Skull Valley are thickest adjacent to the highest parts of the Stansbury Mountains thus supporting Helm's (1995) proposed sections of the Stansbury fault. She postulates that the fault sections are rupture segments that may or may not rupture independently.

South of Johnson Pass, Hecker (1993) also includes a fault trace along the western margin of the Onaqui Mountains mapped by Moore and Sorensen (1979) as part of the Stansbury fault. Sack (1993) also mapped this trace and referred to it as the Onaqui fault zone. This fault extends from Johnson Pass south to a major canyon termed The Delle, a distance of about 9 km. West of The Delle, a bedrock salient extends westward from the base of the Onaqui Mountains, and is crossed by numerous north-trending, discontinuous fault strands (Moore and Sorensen, 1979). South of this salient, the range front is sinuous, and Moore and Sorensen (1979) do not map a fault along the range margin. Sack (1993), however, shows a west-down fault along the southern 3 km of the western Onaqui Mountains front. The range-crest elevations south of Johnson Pass support the presence of at least one additional fault section between Johnson Pass and Lookout Pass.

There is some uncertainty concerning the timing of the most-recent earthquake on the Stansbury fault, although all workers agree that there has been late Quaternary movement. On the basis of fault-scarp morphology, Barnhard and Dodge (1988) and Helm (1995) suggest that the most recent movement on the Stansbury fault occurred prior to the Lake Bonneville highstand (about 15,000 years ago). In contrast, on the basis of stream nickpoints located a short distance upstream of the scarps, Everitt and Kaliser (1980) concluded that the most recent movement on the fault occurred during the Holocene. Barnhard and Dodge (1988) addressed this possibility by visiting two stream channels with prominent nickpoints, and concluded that resistant bedrock influenced upstream migration of the nickpoints, and thus that the fault has not had Holocene displacement. Field mapping by Sack (1993) also suggests the possibility that there has been surface rupture along the fault since the Bonneville highstand. Via analysis of aerial photography, she identified several northwest-trending *en echelon* fault scarps that offset the Bonneville shoreline located about 10 km northeast of Hickman Knolls. In addition, Barnhard and Dodge (1988), and Helm (1995) map a series of *en echelon* fault scarps topographically lower than the Bonneville shoreline. It is unclear why these workers conclude that the most-recent earthquake pre-dates the Bonneville highstand while at the same time acknowledge the presence of these fault scarps. Our field reconnaissance of the scarp at Indian Hickman Canyon, directly east of the PFSF site, supports the interpretation that the Stansbury fault scarp displaces late Quaternary alluvial-fan deposits and has had multiple late Quaternary surface ruptures. We conclude that the Stansbury fault has had recurrent

movement during the middle to late Pleistocene, and perhaps has ruptured since the Bonneville highstand.

Helm (1995) summarizes available scarp-height data along the fault, and shows that the scarps range in height from 3.9 to 49.5 m. Barnhard and Dodge (1988), Hecker (1993), and Helm (1995) all state that scarp heights are greater in older alluvial deposits than in younger deposits along the length of the fault, indicating recurrent movement during the Quaternary (within the past 1.6 million years). Krinitzsky (1989) states that the single-event displacement is 2.4 to 3.9 m, based on data given by Barnhard and Dodge (1988). However, Barnhard and Dodge (1988) note the presence of a 20-m-wide graben along most of the fault trace, and thus reported scarp measurements may overestimate the net tectonic displacement. Barnhard and Dodge (1988) and Helm (1995) caution against using scarp height and surface deformation data to estimate net tectonic displacement.

Slip rates are good indicators of relative fault activity over long time periods, and are critical to the assessment of seismic source characteristics. Unfortunately, there are no published data on the late Quaternary slip rate of the Stansbury fault. Helm (1995) estimates that there has been about 850 m of vertical separation of a basalt flow that is about 12.4 million years old, and calculates a long-term slip rate of 0.07 ± 0.02 mm/yr. This amount of displacement is from the northern section of the fault, north of Pass Canyon, and thus may be slightly lower than the post-12.4 Ma displacement along the southern section. In addition, the Stansbury fault likely dips moderately to the west, and therefore the net slip rate on the fault is probably slightly higher than the vertical separation rate. Other Basin and Range faults that lie west of the Wasatch fault have Quaternary slip rates in the range of 0.1 to 0.2 mm/yr. We use this range to characterize the slip rate for the Stansbury fault. Based on these data, we conclude that the Stansbury fault is a capable tectonic source.

3.2.2 East Cedar Mountains Fault

As part of a hydrologic reconnaissance of Skull Valley, Hood and Waddell (1968) inferred the presence of a fault with east-down displacement along the eastern margin of the Cedar Mountains, herein informally termed the East Cedar Mountains fault (Plate 1). This inferred fault extends from a point due east of Hastings Pass and about 7 km southwest of the village of Delle (along Highway 80), south along the eastern margin of the Cedar Mountains to the

southern end of the range at the town of Dugway. At its closest location, the fault is 9 km from the PFSF site. As shown by Hood and Waddell (1968), the fault contains a northern, 33-km-long section that strikes about N10°E, and a southern, 27-km-long section that strikes about N45°W. The total fault length as shown by Hood and Waddell (1968) is 60 km.

Later workers, concentrating on the presence of fault scarps present in alluvial deposits in the region, did not acknowledge the existence of this fault (Everitt and Kaliser, 1980; Barnhard and Dodge, 1988; Hecker, 1993). However, Arabasz and others (1989) included suspected Pleistocene fault scarps along the northeastern flank of the Cedar Mountains, north of the fault mapped by Hood and Waddell (1968), in their compilation of seismic sources in the region. These possible faults were based on photolineaments that had been identified, but not field checked, by Barnhard and Dodge (1988). Hecker (1993) designates these inferred faults as "Quaternary (?)" and shows them as a 10 km-long zone of short (<2 km) discontinuous fault scarps that are 2 to 3 km east of the range front. Considering these possible fault traces as part of the East Cedar Mountains fault, the fault extends from the northern end of the Cedar Mountains at Interstate 80, to the southern end of the range at the town of Dugway. This interpretation of the fault yields a total fault length of 72 km, with a 45-km-long northern section and a 27-km-long southern section.

The entire length of the East Cedar Mountains fault is within the area covered by the late Pleistocene Lake Bonneville, based on the location of the Bonneville and Provo shorelines mapped by Currey and others (1983), Barnhard and Dodge (1988), and Sack (1993). The possible fault traces at the northern end of the range mapped by Barnhard and Dodge (1988) are located basinward of the 10,000- to 11,000-year-old Gilbert shoreline shown by Sack (1993). This would suggest possible fault movement within the past 11 ka. However, detailed mapping of surficial deposits throughout Skull Valley by Sack (1993) does not show the presence of the possible fault identified by Barnhard and Dodge (1988). It is likely that the features identified by Barnhard and Dodge (1988) are not related to surface faulting.

In addition, Sack (1993) identified a 1.5-km-long, northeast-facing scarp along the eastern margin of the Cedar Mountains, approximately 9 km southwest of Hickman Knolls. This scarp also is basinward of the Provo (<15 ka) shoreline and, if related to surface faulting, would suggest a surface-rupture earthquake within the past approximately 15,000 years.

However, our aerial reconnaissance and preliminary aerial photographic analysis conducted during this study showed no evidence of surface displacement at the location of the scarps noted by Sack (1993), nor anywhere else along the eastern Cedar Mountains range front between Rydalch Canyon and Dugway. Based on examination of aerial photography conducted for this study, the scarps identified by Sack (1993) are at the same elevation as sinuous lake shoreline features to the southwest. Therefore, we interpret that the features mapped by Sack (1993) are shoreline scarps.

Thus, we conclude that there is no definitive evidence of post-Bonneville displacement along the East Cedar Mountains fault, as implied by mapping by Everitt and Kaliser (1980), Barnhard and Dodge (1988), and Hecker (1993). However, with the available data, we cannot preclude the possibility of middle or late Pleistocene displacement (between 500 and 15 ka). Based on the available data, therefore, we conclude that the East Cedar Mountains fault is a potentially capable tectonic source.

3.2.3 West Cedar Mountains Fault

Aerial reconnaissance conducted for this study on September 2, 1996 suggests the presence of a fault along the western margin of the southern Cedar Mountains west of White Rock. At its closest approach, the west Cedar Mountains fault is 19 km from the PFSF site. The fault was mapped by Moore and Sorenson (1979) as an east-vergent thrust fault within Pennsylvanian bedrock. The 8.5-km-long fault is identified based on a southwest-facing bedrock scarp, alignment of topographic saddles, and linear alignment of flowing springs. These features maybe related to the juxtaposition of different rock types along the fault. Because the activity of this inferred fault is unknown, we assume that the west Cedar Mountains fault is a potentially capable fault.

3.2.4 Clover Fault Zone

The Clover fault is a northwest-trending, east-dipping normal fault that borders the northeast flank of the Onaqui Mountains along the western margin of Rush Valley (Bucknam, 1977; Everitt and Kaliser, 1980; Hecker, 1993). This fault zone also is referred to as the North Onaqui East Marginal fault (Everitt and Kaliser, 1980; Krinitzsky, 1989). At its closest approach, the Clover fault zone is 27 km from the PFSF site. Scarps in late Pleistocene to

Holocene(?) alluvium indicate a minimum fault length of 4 to 7 km. The scarps have been modified by agricultural activities and, therefore, cannot be used to estimate the age of faulting. The graded profiles of streams that cross the fault suggest that the most recent faulting occurred more than several thousand years ago (Barnhard and Dodge, 1988). Arabasz and others (1989) assign an age of >15.5 ka to the timing of the last movement on this fault. Scarps heights of 1.1 to 1.2 m, and a single event displacement of 0.6 m, are reported for the Clover fault (Barnhard and Dodge, 1988; Krinitzsky, 1989).

The total length of the Clover fault is uncertain. The fault is one of a series of short discontinuous zones of Quaternary faulting along the western margins of the Tooele and Rush Valleys. To the north, a short (1.3-km-long), east-facing fault scarp in older alluvium near East Hickman Canyon is mapped by Solomon (1993). To the south, prominent Quaternary fault scarps are mapped along the Sheeprock fault (Plate 1). The short lengths of these fault scarps suggest that the earthquakes that produced these scarps were at or near the threshold magnitude of surface rupture (i.e., M 6 to 6.5) and that the length of subsurface rupture may have exceeded the length of surface faulting. Based on the presence of scarps across late Pleistocene and Holocene (?) deposits, we conclude that the Clover fault zone is a capable tectonic source.

3.2.5 Mid-Valley Horst Faults

The Mid-Valley Horst faults border an uplifted structural block within the middle of Rush Valley referred to as the "mid-valley horst" (Everitt and Kaliser, 1980) or the "St. John Station Alluvial Fill faults" (Arabasz and others, 1989). At their closest approach, these faults are 32 km from the PFSF site (Plate 1). The low scarps (0.6 m) and short length (5.6 km and 3.0 km, respectively) along the both the western and eastern margins of the mid-valley horst (Everitt and Kaliser, 1980) suggest that the magnitude of the most recent surface-faulting event was at or near the threshold of surface faulting. Subsurface investigations revealed the presence of additional faults concealed by surficial deposits that are likely related to the mid-valley structure (CH2M Hill, 1986; Jacobs/URS/Blume, 1988). Based on these data, Jack R. Benjamin and Associates (1994) concluded that the total lengths of faults along the western and eastern margins of the mid-valley horst are 5.6 km and 8 km, respectively.

The age of the most recent surface-faulting event on these faults is not known. The scarps that are in both alluvium and gravel-capped pediments of pre-Bonneville age are judged to pre-date the Bonneville highstand (15.5 ka) (Everitt and Kaliser, 1980; Barnhard and Dodge, 1988). Stratigraphic and geomorphic relationships suggest that these faults are late Pleistocene (Hecker, 1993). The faults exposed in trenches at the site by CH2M Hill (1986) are not expressed at the surface. The age of the most recent movement varies among the faults revealed in the trenches. Some of the faults in the Salt Lake Group of late Tertiary age do not extend into overlying Quaternary deposits. The youngest faults exhibit small displacements (suggestive of single events) in the older alluvium but do not appear to displace the soil formed on these deposits that is judged to be approximately 125 ka (Jacobs/URS/Blume, 1988). The maximum post-Salt Lake Group displacement associated with a single fault plane in these trenches was approximately 1.5 m (Krinitzsky, 1989). Smaller displacements of less than 0.3 m are observed on faults that displace the older Quaternary alluvium. Given the evidence for Pleistocene activity, we conclude that these faults are a capable fault source.

3.2.6 Lookout Pass Fault

Moore and Sorensen (1979) map the west-down Lookout Pass fault for a distance of about 6 km along the western margin of the southernmost Onaqui Mountains, south of Lookout Pass. At its closest approach, the Lookout Pass fault is 36 km from the PFSF site (Plate 1). Hecker (1993) suggests that this fault may have had Quaternary displacement, on the basis of the "fault control of bedrock-alluvium contact" (p. 48). Our aerial reconnaissance of the fault showed an absence of prominent geomorphic expression of faulting. Because the activity of this fault is unknown, we assume that the Lookout Pass fault is a potentially capable fault.

3.2.7 Mercur-Topliff Hill Fault Zone

The Mercur-Topliff Hill fault zone consist of a zone of Quaternary faulting along the western side of the Oquirrh Mountains and Topliff Hill in Rush Valley (Plate 1). At its closest approach, this fault zone is 40 km from the PFSF site. This fault zone is aligned with a series of similar major westward-dipping, range-bounding Quaternary normal faults that includes the Oquirrh (Everitt and Kaliser, 1980; Olig and others, 1995) and East Great Salt Lake (Pechman and others, 1987; Viveiros, 1986) fault zones to the north and the East Tintic Mountain fault zones (Barnhard and Dodge, 1988) to the south (Plate 1). In their seismic hazard model,

Youngs and others (1987) treat these faults as individual segments in a large fault zone referred to as the Oquirrh Mountain fault zone. Alternatively, each of these fault zones is described as a separate fault zone in the recent compilation by Hecker (1993).

The Mercur fault zone consists of a 16-km-long alignment of late Pleistocene fault scarps along the western flank of the Oquirrh Mountain in Rush Valley. Based on exposures of faulted alluvium exposed in a mining shaft, together with an uplifted bedrock pediment. Everitt and Kaliser (1980) estimated a minimum of 60 m of Quaternary displacement on the fault. From scarp profile data, the Mercur scarps record displacements of 1.8 to 5.6 m (Barnhard and Dodge, 1988). Solomon (1993) identified a small fault scarp south of the town of Stockton approximately 11 km north of the Mercur fault that exhibits a similar orientation and sense of displacement to the Mercur fault zone scarps. This scarp offsets late Pleistocene Lake Bonneville sediments (15.5 ka), and it is not clear if it is related to surface-faulting events along the Oquirrh fault zone to the north or the Mercur fault zone to the south.

The Topliff Hill fault zone lies along the west flank of the northern East Tintic Mountains, a lower more subdued range to the south of the Oquirrh Mountain range (Hecker, 1993). A zone of fault scarps, which are relatively continuous for a distance of 12 km, exhibit a similar geomorphic position and sense of displacement as those along the Mercur fault zone. These scarps also show evidence for recurrent movement with a cumulative maximum displacement of 5.8 m, but appear to be younger than the Mercur fault scarps based on scarp profile data (Barnhard and Dodge, 1988).

Everitt and Kaliser (1980) concluded that the most-recent surface faulting event along the Mercur-Topliff Hill fault zone post-dated the formation of the Bonneville shoreline and therefore was younger than approximately 14.5 ka. Barnhard and Dodge (1988) reinterpreted a trench log by Everitt and Kaliser (1980), and note that scarps along the Mercur-Topliff Hill fault zone are wave-etched and older than the Bonneville shoreline, and thus are not a result of post-Bonneville surface faulting. Based on scarp morphology the Mercur-Topliff Hill fault zone scarps are interpreted to be late Pleistocene (Barnhard and Dodge, 1988; Hecker, 1993). Based on the presence of scarps across and observed displacement of late Pleistocene deposits, we conclude that the Mercur-Topliff Hill fault zone is a capable tectonic source.

3.2.8 Sheeprock Fault Zone

The Sheeprock fault is a northeast- to northwest-trending, east-dipping normal fault along the northeastern flanks of Sheeprock Mountain. At its closest approach, the Sheeprock fault is 41 km from the PFSF site. A zone of Quaternary fault scarps extend about 10 to 11 km along the fault zone (Everitt and Kaliser, 1980; Barnhard and Dodge, 1988; Hecker, 1993; Bucknam, 1977). Scarp heights range from 1.9 to 16.5 m with some scarps representing repeated surface rupture (Barnhard and Dodge, 1988). A possible Holocene age was inferred for the most-recent event along the Sheeprock fault (Everitt and Kaliser, 1980). However, more recent scarp-profile investigations suggest that the Sheeprock scarps appear to be older than the Topliff Hill, Mercur, and Stansbury scarps, all of which are recognized to pre-date the Bonneville highstand (15.5 ka) (Barnhard and Dodge, 1988). Diffusion-equation modeling of the scarps yielded an age of about 53 ka for the scarps (Hanks and others, 1984). The embayed character of the range front suggests a long period of activity preceding the recent episode of faulting (Everitt and Kaliser, 1980). We conclude that the Sheeprock fault zone is a potentially capable tectonic source.

3.2.9 Oquirrh Fault Zone

The Oquirrh fault zone is a west-dipping normal fault that borders the western side of the Oquirrh Mountains in Tooele Valley. At its closest approach, the Oquirrh fault zone is 45 km from the PFSF site. A variety of names have been used for this fault zone including: the Oquirrh marginal fault (Everitt and Kaliser, 1980); the northern Oquirrh fault zone (Barnhard and Dodge, 1988; Hecker, 1993); and the Oquirrh fault zone (Olig and others, 1995). We follow Olig and others (1995) in referring to the zone of Quaternary faulting along the northern part of the Oquirrh Mountains as the Oquirrh fault zone. The fault zone extends for a least 21 km and has been subdivided into two sections: a northern section that includes fault scarps in alluvium, and a southern section that includes a fault contact between bedrock and alluvium along the range front (Everitt and Kaliser, 1980; Barnhard and Dodge, 1988). An additional segment near Silcox Canyon southwest of Tooele, identified by Everitt and Kaliser (1980) as a scarp of erosional or undetermined origin is identified by Solomon (1993) as a fault scarp.

Scarps along the Oquirrh fault zone range in height between 2.9 and 10.8 m, and surface offsets are between 1.3 and 7.3 m (Barnhard and Dodge, 1988). Locally, the compound scarps

represent displacement during more than one surface-faulting earthquake. Scarps of the Oquirrh fault zone displace the Provo shoreline of Lake Bonneville. Studies of scarp morphology suggest that the most recent surface-faulting event occurred between 9 and 13.5 ka (Everitt and Kaliser, 1980; Barnhard and Dodge, 1988). More recently, paleoseismological investigations along the northern section of the Oquirrh fault zone by Olig and others (1995) documented that: (1) the most recent surface faulting event occurred between 4.3 and 6.9 kyr B.P., (2) the second-most-recent event occurred between 20.3 and 26.4 kyr B.P., (3) the net vertical tectonic displacement is between 1.9 and 3.3 m with best estimates of 2.2 and 2.7 m for the most-recent event and 2.3 m for the penultimate event, (4) the recurrence interval between the last two events ranges from 13.3 and 22.1 kyr B.P., (5) calculated slip rates are 0.1 to 0.2 mm/yr for this interval, and (6) the third-most-recent event probably occurred before 33.95 ± 1.16 kyr B.P.

Total length of the Oquirrh fault zone is estimated to be 35 km, which allows for the fault to extend a few kilometers northwards into the Great Salt Lake and includes the isolated, short, discontinuous fault scarps near Stockton. Comparison of the available information regarding timing of the surface-faulting events on the Oquirrh fault zone, and the Mercur fault zone to the south suggests that these fault zones have behaved as independent rupture segments since the Bonneville lake cycle (Olig and others, 1995). Available paleoseismic information is inconclusive regarding a possible rupture segment boundary between the Oquirrh fault zone and the East Great Salt Lake fault zone to the north (Olig and others, 1995). We conclude that the Oquirrh fault zone is a capable tectonic source.

3.2.10 Vernon Hills Fault Zone

The Vernon Hills fault zone is a 5- to 7-km-long, northwest-trending, normal fault within Rush Valley (Everitt and Kaliser, 1980; Bucknam, 1977). At its closest approach, the Vernon Hills fault zone is 47 km from the PFSF site. Along most of the zone, bedrock occurs on both sides of the fault or is juxtaposed against alluvium (Barnhard and Dodge, 1988). Based on scarp morphology and shoreline relations, the most-recent surface-faulting earthquake on the Vernon Hills fault zone appears to pre-date the Bonneville shoreline and therefore is older than 15.5 ka. Scarp heights of 3.3 to 4.3 m and surface offsets of 1.7 to 2.3 m are reported by Barnhard and Dodge (1988). Hecker (1993) designates the fault zone as late Pleistocene. We conclude that the Vernon Hills fault zone is a capable tectonic source.

3.2.11 Lakeside Mountains Fault

A possible Quaternary fault is shown by Anderson and Miller (1979) along the western flank of the Lakeside Mountains, based on an inferred fault control of the bedrock-alluvium contact (Moore and Sorensen, 1979; Young, 1955). The fault as shown by Hecker (1993) is 5 km long. At its closest distance, the fault is 49 km from the PFSF site. Arabasz and others (1989) included the fault (queried as to state of activity) in a compilation of seismic sources in the region. They reference T. P. Barnhard (person. commun., 1987) as having identified the feature as a lineament that may be a shoreline feature. The fault does not appear on the maps of Bucknam (1977) or Barnhard and Dodge (1988). Based on the uncertainty in fault existence and recency of activity, we conservatively judge the fault to be a potentially capable tectonic source.

3.2.12 Simpson Mountains Fault

The Simpson Mountains fault is a northwest-trending, west-dipping fault within the narrow basin to the southwest of the Simpson Mountains. At its closest approach, the Simpson Mountains fault is 52 km south of the PFSF site. Scarps in alluvium southwest of the Simpson Mountains identified by Ertec Western, Inc. (1981) are designated as middle to late Pleistocene (10,000 to 750,000 years) faults by Hecker (1993). The approximately 10-km-long zone of discontinuous scarps are not associated with a well-defined or linear range front. As mapped by Hecker (1993), individual scarps are generally less than 2 km long.

3.2.13 Sheeprock Mountains Fault

The Sheeprock Mountains fault is a northwest-trending, west-dipping fault that borders the western margin of the Sheeprock Mountains (Plate 1). At its closest approach, the Sheeprock Mountains fault is 57 km southeast of the PFSF site. Based on faulted alluvial-fan deposits, Ertec Western, Inc. (1981) identified this fault as having early Pleistocene movement. Although this fault is designated as an early to middle Pleistocene (130,000-1,650,000 years) fault by Hecker (1993), the age of movement, which is based primarily on the age of faulted deposits, is considered a maximum estimate. The fault is located in piedmont alluvial fan deposits approximately 2 to 3 km from the range front. The total length of the fault as shown

by Hecker (1993) is approximately 4.5 km. We consider the Sheeprock Mountains fault as a potential capable source.

3.2.14 Puddle Valley Fault Zone

The Puddle Valley fault zone is comprised of a group of fault scarps that extend for a distance of approximately 6 km along the western margin of Puddle Valley, a few kilometers east from the relatively subdued range front of the Grassy Mountains. At its closest approach, the Puddle Valley fault zone is 61 km northwest of the PFSF site. The fault scarps, which are topographically below the Bonneville and Provo shorelines, may represent two spatially distinct surface-rupturing events (Barnhard and Dodge, 1988). On the basis of scarp morphology, scarps at the north end of Puddle Valley appear to be older than the Bonneville shoreline: those at the south end appear to be younger than the Bonneville shoreline but older than the Drum Mountains fault scarps in southern Utah, which have been estimated to be 9,000 years old (Pierce and Colman, 1986). Based on the studies of Barnhard and Dodge (1988), Hecker (1993) suggests that the age of most recent movement is 9 to 15? ka, and the displacement per event is 0.7 to 2.3? m. We conservatively conclude that the Puddle Valley fault zone is a capable tectonic source.

3.2.15 East Great Salt Lake Fault Zone

Gravity and seismic reflection data indicate that a major 82-km-long zone of faulting is concealed beneath the Great Salt Lake along the western margin of the NNW-trending linear topographic high that includes the Promontory Mountains, Fremont Island, and Antelope Island. This west-dipping fault, named the East Great Salt Lake fault zone by Cook and others (1980), is clearly delineated in seismic reflection profiles across the lake (Viveiros, 1986; Mukulich and Smith, 1974; Smith and Bruhn, 1984). At its closest approach, this fault zone is 66 km northeast of the PFSF site. This fault cuts sediments identified as Quaternary based on well data and appears to displace sediments within 10 to 20 m of the lake bottom (Viveiros, 1986; Hecker, 1993; Mukulich and Smith, 1974). A 1.5-km-long zone of *en echelon* fractures beneath the lake west of Antelope Island appears on aerial photos to have slight down-to-the-west displacement and to be unmodified by coastal processes, and thus may date from the latest Holocene (Smith and Bruhn, 1984; Hecker, 1993). A zone of subsidiary faults lies within about 5 km west of the main fault in the southern Great Lake (Hecker, 1993). These

faults may represent the northern extension of the Oquirrh fault zone. The relationship between the Oquirrh and East Great Salt Lake fault zones is not well delineated on the compilation map presented by Hecker (1993). We consider the East Great Salt Lake fault as a capable tectonic source.

3.2.16 East Tintic Mountains Fault

The 36-km-long East Tintic Mountains fault is a north-trending, west-dipping fault along the western side of the East Tintic Mountains (Plate 1). At its closest approach, this fault is 72 km southeast of the PFSF site. Isolated, highly dissected scarps in alluvium along the fault appear to be among the oldest in western Utah (Bucknam and Anderson, 1979). Anderson and Miller (1979) mapped buried Quaternary (?) faults extending to the north and south of the alluvial scarps. These faults and faults that form bedrock-alluvium contacts at the south end of the East Tintic Mountains (Morris, 1987) are mapped as Quaternary (?) by Hecker (1993). This fault zone was considered to be a segment of the Oquirrh fault zone as described by Youngs and others (1987). Given the differences in recency and activity along this fault compared with the Mercur-Topliff Hill, Oquirrh, and East Great Salt Lake fault zones to the north, we consider this fault as an independent potentially capable tectonic source.

3.2.17 West Valley Fault Zone

The West Valley fault zone consists of a series of mostly east-dipping normal faults that displace late Quaternary lake deposits in Salt Lake Valley (Plate 1). At its closest approach, the West Valley fault zone is 75 km northeast of the PFSF site. This fault zone was originally called the Jordan Valley fault zone and subsequently renamed the West Valley fault zone (Keaton and others, 1987). The southern portion of the fault zone consists of two subparallel east-facing scarps (the Granger and Taylorsville faults), whereas the northern portion is broader and is characterized by many smaller, east- and west-facing scarps. Locally, the near-surface expression of the fault zone is characterized by monoclinial flexuring and minor step-faulting. The total length of the zone is about 18 km (Keaton and others, 1987). Geomorphic and stratigraphic evidence of two events in the past 12 to 13 ka is documented along the main Granger and Taylorsville faults (Keaton and others, 1987). Geomorphic relations within the northern West Valley fault zone suggest that four or more events occurred in the same time period and that some of the post-Bonneville faulting occurred prior to formation of the Gilbert

shoreline (12 ka). Borehole evidence associated with several traces of the northern West Valley fault zone suggests that the most recent event may have occurred 6 to 9 ka and that two or three events may have occurred since 22 to 28 ka (Hecker, 1993; Keaton and others, 1987). As noted by Youngs and others (1987), it is unclear whether movement on the West Valley fault zone is independent or directly tied to movement on the Salt Lake City segment of the Wasatch fault zone. A Holocene slip rate of 0.5-0.6 mm/yr is estimated for the Granger fault and the West Valley fault zone as a whole. Lower rates of 0.1 to 0.2 mm/yr are inferred for the Taylorsville fault over longer periods of time (< 140 ka). The relatively high slip rate calculated for post-Bonneville time suggests that strain release may be due to isostatic rebound within an extensional setting (Hecker, 1993). We consider the West Valley fault zone as a capable tectonic source.

3.2.18 East Lakeside Mountains Fault Zone

A major 38-km-long Quaternary (?) fault is identified in the Great Salt Lake along the eastern margin of the Lakeside Mountains based on gravity and seismic-reflection profile data. At its closest approach, the East Lakeside Mountains fault zone is 78 km north of the PFSF site. This major structure borders the west side of the Great Salt Lake graben (Plate 1). Seismic reflection data indicates that faulting extends up into Quaternary deposits, although the activity of the fault is undetermined (Hecker, 1993). We consider this fault zone as a potential capable source.

3.2.19 Utah Lake Fault Zone

Latest Pleistocene to Holocene(?) faults and associated folds are identified over a 30 km length in Utah Lake based on seismic-reflection profile data (Brimhall and Merritt, 1981). At their closest approach, the Utah Lake faults are 79 km east of the PFSF site. Due to the widely spaced seismic-reflection transects, the fault locations are uncertain. An 8- to 15-m-deep layer identified as the Provo Formation, which is interpreted to be lake bottom sediments probably deposited during the regressive phase of Lake Bonneville (Machette, 1989), is displaced from < 2 to 5 m across individual faults and folds beneath the lake. The reflection profiles suggest that displacements decrease upward in strata above this horizon and occur within several meters of the lake bottom. Based on the uncertainties in the geometries and tectonic

significance of these structures, we consider the Utah Lake fault zone to be a potential capable source.

3.2.20 Drum Mountains Fault Zone

The Drum Mountains fault zone is a series of north-trending, east-dipping faults along the eastern margin of the Drum Mountains. At its closest approach, the fault zone is 80 km south of the PFSF site. Bucknam and Anderson (1979) map a 5-km-wide zone of fault scarps within pre-Lake Bonneville age deposits east of the Drum Mountains. The fault zone, as shown by Hecker (1993), is 36 km long. Faulted Provo-level shoreline features provide a maximum age of 13.5 ka for the scarps (Crone, 1983). Scarps range in height from 0.7 to 7.3 m, with average heights of 2.4 m, and show no geomorphic evidence of having multiple events (Hanks and others, 1984). Morphometric analyses of the scarps provide ages of 5.6 ka (Hanks and others 1984) and 9 ka (Pierce and Colman, 1986). Trenching by Crone (1983) showed that Holocene faulting produced 3.7 m of stratigraphic throw, significantly more than the 2.7 m of surface offset measured from nearby scarp profiles. We consider the Drum Mountains fault zone as a capable tectonic source.

3.2.21 Fish Springs Fault

The Fish Springs fault is a north-trending, east-dipping fault along the eastern margin of the Fish Springs Range. At its closest approach, the fault is 81 km southwest of the PFSF site. Bucknam and Anderson (1979) map the Fish Springs fault within alluvial fan deposits near the eastern base of the Fish Springs Range. The fault consists of a single trace about 8 km long, and a northern fault trace about 3 km long. The potential fault rupture length, assuming scarps along both traces represent surface rupture in a single event, is about 12 km long (Bucknam and Anderson, 1979). A lack of scarp dissection and sharp nickpoints in small washes that cross the scarps suggest that the fault scarps are young (Bucknam and Anderson, 1979). The scarps occur below the level of the Bonneville shoreline and offset alluvial fan deposits that overlie shoreline features. The scarps therefore are younger than 12 ka. Field observations by Bucknam and Anderson (1979) suggest a maximum single-rupture surface offset of 3.3 m. We consider the Fish Springs fault as a capable tectonic source.

3.2.22 Wasatch Fault Zone

The Wasatch fault zone is a major 370-km-long structural feature that forms the eastern boundary of the Basin and Range province east of the PFSF site (Plate 1). The Wasatch fault zone contains nine westward-dipping normal fault segments that exhibit late Pleistocene or younger activity (Hecker, 1993). These segments are differentiated on the basis of timing of individual earthquakes and changes in scarp morphology and geometry (Machette and others, 1991). Three of the Holocene segments of the Wasatch fault zone are located within 100 km of the PFSF site: the Salt Lake City, Provo, and Nephi segments. Paleoseismologic studies show that there have been repeated large-magnitude earthquakes on all three of these segments of the Wasatch fault zone. A seismic source model for these segments is provided by Youngs and others (1987).

The 46-km-long Salt Lake City segment of the Wasatch fault zone is located approximately 81 km east of the PFSF site. The Salt Lake City segment consists of three left-stepping surface traces that bound the western base of the Wasatch Range within Salt Lake City (Machette and others, 1991). The most-recent earthquake on the segment probably occurred 1,000 to 1,800 years ago (Hecker, 1993). However, diffusion-equation modeling of scarp degradation suggests a more recent age of 900 years. Based on Holocene fault scarps, average surface displacement per event is 2 m. Latest Quaternary slip rate estimates of 1 mm/yr are assigned to this segment of the Wasatch fault zone (Hecker, 1993).

The 70-km-long Provo segment of the Wasatch fault zone borders the eastern margin of Utah Valley, approximately 98 km northeast of the PFSF site. The most-recent earthquake on the Provo segment likely occurred 500 to 650 years ago based on recent trenching (Machette and others, 1991). Six or seven post-Provo events yield an average recurrence interval of 1,700 to 2,600 years for major earthquakes (Hecker, 1993). Up to 3 m of surface offset per earthquake is estimated for this segment (Machette and others, 1991). Slip rate estimates for the segment vary between 1 and 1.7 mm/yr (Hecker, 1993).

The 43-km-long Nephi segment of the Wasatch fault zone, located approximately 99 km from the PFSF site, is the southernmost fault segment that shows evidence of repeated Holocene movement. The Nephi segment extends from Nephi to Payson and is separated from the Levan segment of the Wasatch fault zone to the south by a 15-km-long gap containing no

evidence of faulting (Machette and others, 1991). The Nephi segment is one of the most recently active segments, with scarp morphology suggesting displacement occurred approximately 300 to 500 years ago, although radiocarbon dates suggest an age of about 1,200 for the most-recent earthquake (Hecker, 1993). Middle to late Holocene recurrence intervals for major earthquakes may vary between less than 1,000 years to more than 3,000 years. Provo sediments are offset as much as 2 m along the Nephi segment. Slip rates along the segment range from 0.8 to 1.3 mm/yr, decreasing from north to south (Hecker, 1993).

3.2.23 West Deep Creek Fault

Barnhard and Dodge (1988) mapped the Deep Creek fault along the western margin of the Deep Creek Mountains. At its closest approach the West Deep Creek fault is 99 km southwest of the PFSF site. The 12-km-long fault offsets Quaternary basin-fill gravelly sands down to the west. The southernmost 6-km-long extension of the fault is mapped based on alignment of vegetation lineaments and springs (Barnhard and Dodge, 1988). Surface faulting is probably pre-Bonneville highstand (>15 ka) based on comparison of scarp profiles across the northern half of the fault (Barnhard and Dodge, 1988). Scarps show evidence for multiple episodes of movement with measured cumulative displacements between 1.7 and 3.4 m (Hecker, 1993). We consider the West Deep Creek fault as a capable tectonic source.

3.3 Other Mapped Features in the Vicinity of the Skull Valley Site

3.3.1 "Hickman Knolls Fault and Lineament Zone"

Directly north of Hickman Knolls, Sack (1993) mapped a series of subparallel lineaments in Sections 5, 6, 7, and 8 (T.5S., R.8W.), and referred to the features as the "Hickman Knolls fault and lineament zone". The lineaments occur in a zone that is about 1.5 km wide and 2 km long, and were identified via analysis of 1:60,000-scale aerial photography. The lineaments are evenly spaced at intervals of about 100 m, and all are located directly south of a prominent, west-trending shoreline interpreted as the Stansbury shoreline by Sack (1993). Sack (1993) notes that the lineaments occur within lacustrine fine-grained deposits on the valley floor, and that one lineament extends across "mixed lacustrine and alluvial deposits" and colluvium in the Hickman Knolls. Analysis of aerial photography suggested to Sack (1993) that a possible scarp along this lineament was small.

Our aerial reconnaissance, analysis of small-scale (1:20,000- and 1:40,000-scale) aerial photography, and field investigations confirm the presence of this series of lineaments directly north of Hickman Knolls. Our field studies included reconnaissance of the lineament that extends into the colluvial deposits in Hickman Knolls, and of the lineaments north of Hickman Knolls. The single lineament present in the Hickman Knolls is located along a small, north-trending swale that has developed parallel to bedding within the dolomite bedrock composing the Hickman Knolls. It appears likely that the swale is related to differential erosion of units within the bedrock. The swale projects toward, but is not continuous with, the lineaments present in fine-grained lacustrine deposits further to the north. In addition, there are several wave-cut notches developed on the bedrock that can be traced along the northern margin of Hickman Knolls and that show no change in elevation across the southern projections of any of the lineaments. Considering that the elevation of the Provo and Bonneville shorelines in the southern part of Skull Valley are higher than the top of Hickman Knolls, these notches likely are related to transgressions or regressions closely before or after the development of the Bonneville or Provo shorelines (<15 ka). Thus, we interpret these relations as evidence that the lineament identified by Sack (1993) within Hickman Knolls is not related to surface faulting.

Our field reconnaissance of the lineaments directly north of Hickman Knolls shows that they are composed of linear, asymmetric ridges of sand and silt having approximately 1 m of relief between each ridge crest and adjacent trough. In general, the western sides of the ridges have slightly steeper slopes than the eastern sides, although each ridge crest plunges gently to the north and the regional topographic slope is northerly. Inspection of 1:24,000-scale topographic maps having a contour interval of 3.3 m (10 ft) shows negligible relief across the entire zone of lineaments, which suggests a lack of tectonic displacement. Our analysis of 1:40,000-scale black-and-white aerial photography shows that the westernmost lineaments are curvilinear and merge together to the north, where they are adjacent to the Stansbury shoreline mapped by Sack (1993). The Stansbury shoreline developed at about 20 to 23 ka, during a lake highstand that preceded the Bonneville shoreline (Currey and others, 1983). In addition, our analysis of aerial photography shows that a broad, but still distinct, lineament south of and subparallel to the mapped Stansbury shoreline obliquely traverses the north-trending lineaments identified by Sack (1993). This lineament extends to the west into Section 7

(T.5S., R.8W.), and coincides with a 1- to 2-m-high curvilinear ridge of lacustrine pebble gravel. There is no displacement of this ridge or pebble gravel across the zone of lineaments mapped by Sack (1993).

On the basis of our aerial reconnaissance, analysis of aerial photography, and field reconnaissance, we interpret that the lineaments present directly north of Hickman Knolls are related to lacustrine processes during previous lake highstands, rather than as a result of surface faulting as postulated by Sack (1993). The asymmetry of the ridges, the curvilinear pattern of the westernmost lineaments, and the proximity to the topographically high Hickman Knolls (which were a rocky peninsula during intermediate lake levels) suggest that the ridges are related to complex near-shore sediment transport. When the lakeshore was in the vicinity of Hickman Knolls, the area now containing the lineaments was a small, concave-north bay between the northeastern margin of Hickman Knolls and bedrock knobs directly to the northeast (Sack, 1993). We believe that the lineaments formed after the development of the Stansbury shoreline, as a result of lake regression following the Provo highstand. The ridges appear to be superimposed on deposits associated with the Stansbury shoreline, which probably influenced near-shore sediment transport and deposition within the small, north-facing the bay. Currey (1996) also conducted an investigation of the lineaments north of Hickman Knolls. Based on field reconnaissance, analysis of shallow soil samples, and examination of aerial photographs, he reached a similar conclusion that they formed by lacustrine processes and are not tectonic in origin.

3.3.2 "Northwest Hickman Knolls Lineament Zone"

Sack (1993) also notes the presence of several northwest-trending lineaments located about 6 km northwest of Hickman Knolls, and notes that they trend across the lower piedmont of the Cedar Mountains. These lineaments are within a zone that is about 1.5 km wide and 5 km long, and are in an area mapped by Sack (1993) as underlain by lacustrine and alluvial sediments. Although Sack (1993) maps these features as "Faults or fractures having small or undetermined displacement," her text refers to them as lineaments rather than faults or fractures. Because of the proximity of these features to the PFSF site, our aerial reconnaissance included an overflight of the area containing these features. However, this reconnaissance failed to reveal any prominent lineaments in the vicinity that could be ascribed to tectonic surface rupture. In addition, our analysis of 1:40,000-scale aerial photography

showed no prominent lineaments in the vicinity. Analysis of the 1:24,000-scale Hickman Knolls orthophotoquad published by the U.S. Geological Survey similarly revealed no evidence of prominent, fault-related lineaments. The orthophotoquad reveals the presence of a distinct, west-trending shoreline or beach ridge that would be crossed by the lineaments mapped by Sack (1993). There is no evidence of deformation of this shoreline by the mapped lineaments. We conclude that there is no evidence to suggest that the "northwest Hickman Knolls lineament zone" mapped by Sack (1993) is related to tectonic surface rupture.

3.3.3 "Springline Fault"

Rigby (1958) interpreted the presence of a fault beneath alluvium along the eastern edge of Skull Valley between Iosepa and Timpie, based on an alignment of bedrock outcrops and warm saline springs. Hood and Waddell (1968) and Helm (1995) also mapped the 18-km-long fault based on the position of the springs. However, Quaternary geologic mapping by Sack (1993) does not show the inferred fault. A possible nontectonic explanation for the linearity of the springs is intersection of the groundwater table with the Gilbert shoreline mapped by Sack (1993). No geomorphic evidence of surface faulting was observed during our aerial and field reconnaissance conducted for this study on September 2 and 3, 1996. We conclude that the Springline fault is not a capable tectonic source.

3.4.4 Faults Identified by Geosphere Midwest (1997)

Geosphere Midwest (1997) performed a seismic reflection study in the site vicinity. They identified numerous possible faults in bedrock in the general vicinity of the "Hickman Knolls fault and lineament zone" mapped by Sack (1993) and addressed in Section 3.3.1 above. Within the limited resolution of the data, Geosphere Midwest (1997) does not interpret these possible bedrock faults to extend into the overlying sediments. Based on the geomorphic evidence supporting a nontectonic lacustrine origin for the Hickman Knolls fault and lineament zone (Curry, 1996), we conclude that the bedrock faults identified by Geosphere Midwest (1997) are not related to the lineament zone. There is no evidence that the bedrock faults identified by Geosphere Midwest (1997), if present, have been active in the Quaternary. Based on the absence of geomorphic and stratigraphic evidence of activity, we conclude that the possible bedrock faults identified by Geosphere Midwest (1997) are not a capable tectonic source.

**TABLE 3-1
POTENTIAL CAPABLE FAULTS
WITHIN 100 KM OF PFSF SITE**

Fault	Distance from PFSF Site	Length (km)	Activity*
Stansbury fault	9.5	73	LP
East Cedar Mountains fault	9	72	Q(?)
West Cedar Mountains fault	19	8.5	Q(?)
Clover fault zone	27	4 to 7	LP
Mid-Valley Horst faults	32	6	LP
Lookout Pass fault	36	6	Q(?)
Mercur-Topliff Hill fault zone	40	16	LP
Sheeprock fault zone	41	10 to 11	LP
Oquirrh fault zone	45	21	H-LP
Vernon Hills fault zone	47	5 to 7	LP
Lakeside Mountains fault zone	49	5	Q(?)
Simpson Mountains fault	52	10	MP-LP
Sheeprock Mountains fault	57	4.5	EP-MP
Puddle Valley fault zone	61	6	H-LP
East Great Salt Lake fault zone	66	82	H-LP
East Tintic Mountains fault	72	36	MP-LP
West Valley fault zone	75	18	H-LP
East Lakeside Mountains fault zone	78	38	Q(?)
Utah Lake faults	79	30	H-LP
Drum Mountains fault zone	80	36	H-LP
Fish Springs fault	81	12	H-LP
Wasatch fault zone		370	H-LP
Salt Lake City segment	81	46	H-LP
Provo segment	98	70	H-LP
Nephi segment	99	43	H-LP
West Deep Creek fault	99	12	LP

* Activity based on Hecker (1993).

H-LP	Holocene to latest Pleistocene (0-30,000 yrs)
LP	Latest Pleistocene (10,000-30,000 yrs)
MP-LP	Middle to late Pleistocene (10,000-750,000 yrs)
EP-MP	Early to middle Pleistocene (130,000-1,650,000 yrs)
Q(?)	Quaternary (?) (<1,650,000 yrs)

4.0 DETERMINISTIC GROUND MOTION ASSESSMENT

This study provides a deterministic assessment of the level of ground motions at the Skull Valley PFSF site, using methodologies prescribed by Appendix A to 10 CFR Part 100 and associated guidance documents (e.g., SRP's, Regulatory Guides). The methodology for certain elements has been established by precedent in application of Appendix A (e.g., use of 84th-percentile ground motion levels). The deterministic procedure follows four steps: (1) assessment of capable faults and seismic sources, (2) evaluation of the closest approach of the faults/sources to the site, (3) assessment of maximum earthquake magnitudes for each fault/source, and (4) estimation of ground motions at the site. The fault/source that gives rise to the largest ground motions at the site is deemed the "controlling" source. Section 3.0 discusses the faults in the region that have been identified as capable or potentially capable seismic sources. Two of these sources, the Stansbury (capable) and East Cedar Mountains (potentially capable) faults lie within 10 km of the site and potentially dip beneath the site. The remaining faults identified in Section 3 (Table 3-1) lie at distances of 20 km or greater from the site and are unlikely to produce 84th percentile ground motion levels that are as large as those that would be estimated for these two faults. Therefore, they will not be characterized further. A third seismic source, the potential for a random near by earthquake unassociated with any mapped fault, also is considered.

4.1 Maximum Earthquakes

4.1.1 Approach

The maximum earthquakes associated with the Stansbury and East Cedar Mountains faults are evaluated by assessing the maximum dimensions of rupture for an individual earthquake on each of the faults and then employing empirical relationships between earthquake rupture dimensions and earthquake magnitude developed by Wells and Coppersmith (1994). The rupture dimensions used are maximum rupture length and maximum rupture area. We also consider the use of the relationship developed by Anderson and others (1996), which relates earthquake magnitude to fault slip rate and rupture length. Because these assessments are uncertain, they are specified in terms of probability distributions rather than single values. The resulting uncertainty in maximum magnitude is propagated through ground motion assessment.

Assessment of the maximum rupture lengths is specific to the individual fault. The assessment of the maximum rupture area is obtained by multiplying the maximum rupture length by the maximum rupture width, which is calculated based on the thickness of the seismogenic crust and the dip of the fault. Seismicity data provides the best indication of the thickness of the seismogenic crust in a region (Sibson, 1982, 1984). The data for faults in the Basin and Range province indicates that the largest events nucleate at depths of about 15 km (Smith and others, 1983). Figure 4-1 shows east-west cross sections of the focal depth distribution of earthquakes in the region. The data indicate that most of the earthquakes occur shallower than about 18 km, with some as deep as 25 km. We consider the thickness of the seismogenic crust to be uncertain within the range of 15 to 20 km. The discrete probability distribution of 15 km (0.4), 18 km (0.4), and 20 km (0.2) was used to express this uncertainty. The depths of 15 and 18 km are favored because of the typical depth of large Basin and Range earthquakes and nearly all of the seismicity occurs shallower than 18 km.

Specific data is not available on the dip of the Stansbury and East Cedar Mountains faults. However, most large normal faulting earthquakes in the Basin and Range province have occurred on fault planes with dips in the range of 45° to 65° (Smith and others, 1983). We represent the uncertainty in the fault dip by considering three equally likely values of 45°, 55°, and 65°.

Because the Stansbury and East Cedar Mountains faults dip toward each other and lie about 18 km apart, the faults potentially intersect at depth, depending upon the fault dips. We assume that the Stansbury fault is the dominant fault because it is much more clearly expressed. Thus the maximum depth of the East Cedar Mountains fault is assumed to range from 9 to 20 km, depending on the dip of the two faults.

4.1.2 Maximum Rupture Lengths

Stansbury Fault

The surface trace of the Stansbury fault is considered to have a total length of 73 km, extending from the northern end of the Stansbury Mountains near the village of Timpie, to Lookout Pass at the southern end of the Onaqui Mountains (Figure 4-2). The fault sections identified by Helm (1995) are used herein with minor modifications, including a 24-km-long section from Timpie south to Pass Canyon (Section "A" herein), and a 23-km-long section

from Pass Canyon to Johnson Pass (Section "B" herein). In addition, we consider the possibility of additional fault sections south of Johnson Pass on the basis of the mapped fault trace and linear range front between Johnson Pass and The Delle, the substantial relief of the Onaqui Mountains, and the fault trace at the southern end of the range mapped by Sack (1993). We identify fault section "C", which extends from Johnson Pass to The Delle and is 9 km long. We also consider fault section "D", which extends from The Delle to Lookout Pass and is 17 km long (Figure 4-2).

We consider five rupture scenarios for the maximum-magnitude earthquake that incorporate various combinations of the four fault sections noted above. Because of the prominence of fault scarps across late Quaternary alluvial deposits along the Stansbury fault between Pass Canyon and Johnson Pass, as well as the proximity of this section, each of the scenarios includes rupture of section "B". The relatively short rupture of 23 km, in which section "B" ruptures alone, is given a low weight (0.1), because it is likely that the maximum earthquake includes rupture along at least one other section. Scenarios that include rupture of section "B" and an adjacent section are given higher probabilities, including a weight of 0.2 for the 47 km-long rupture of sections "A" and "B", and a weight of 0.3 for the 32-km-long rupture of sections "B" and "C". The 56-km-long scenario in which all three of the northern sections ("A", "B", and "C") rupture is weighted 0.3, based on the presence of evidence of recurrent displacement along all three sections. Lastly, the longest scenario, in which rupture occurs along all four sections of the entire 73-km-long fault, is weighted low (0.1) because of the discontinuity of the fault between The Delle and Lookout Pass.

The assessment of maximum magnitude is based on empirical relationships between magnitude and rupture length, and magnitude and rupture area (Wells and Coppersmith, 1994) and the relationship of Anderson and others (1996) between magnitude, rupture length, and slip rate. These relationships are weighted equally in our analysis. The relationships between magnitude and single-earthquake displacement are not used in this analysis because the scarp height data collected along the fault do not necessarily reflect amounts of net tectonic displacement (Barnhard and Dodge, 1988; Helm, 1995). The maximum magnitude distribution includes all five of the rupture scenarios and reflects the postulated rupture dimensions based on combinations of rupture lengths and widths. As discussed in Section 3.2.1, the estimated slip rate of the Stansbury fault is in the range of 0.1 to 0.2 mm/yr.

We represent the uncertainty in slip rate with the discrete distribution of 0.1 mm/yr (0.3), 0.15 mm/yr (0.5), 0.2 mm/yr (0.2), slightly favoring the lower slip rate estimated from fault-specific data.

East Cedar Mountains Fault

The East Cedar Mountains fault is considered to be potentially capable. We define the fault trace to have a total length of 72 km, extending from the northern end of the Cedar Mountains at Interstate 80, to Dugway at the southern end of the Cedar Mountains (Figure 4-2). As discussed in Section 3.2.2, the fault is not clearly expressed in the surface geology. We consider three possible values for the maximum rupture length, 27, 45, and 72 km. A maximum rupture length of 27 km represents the shortest straight segment of the fault and is comparable to the most well expressed segment of the Stansbury fault across Skull Valley. A maximum rupture length of 45 km represents the longest segment of the postulated fault. These two values of maximum length are given the most weight, 0.4 and 0.5, respectively, because they are representative of maximum rupture lengths assessed for the Stansbury fault. Rupture of the entire postulated length of the fault is given a weight of 0.1 because it is considered to be no more likely than rupture of the entire Stansbury fault. No slip rate data were available for the East Cedar Mountains fault.

4.1.3 Maximum Magnitude Assessments

Maximum earthquake magnitudes were computed for the Stansbury and East Cedar Mountains faults using the distributions of maximum rupture parameters described above and published empirical relationships between coseismic rupture dimensions and moment magnitude, M . The selected relationships were the relationship between subsurface rupture length and M and rupture area and M published by Wells and Coppersmith (1994) and the relationship between rupture length, fault slip rate, and M published by Anderson and others (1996). The relationships were weighted equally in computing possible maximum magnitudes. The resulting maximum magnitude probability distributions for the Stansbury and East Cedar Mountains faults are shown on Figure 4-3. The maximum magnitude distribution for the Stansbury fault ranges from moment magnitude M 6.5 to 7.5, with a mean value of 7.0. The assessment for the postulated East Cedar Mountain fault ranges from M 6.5 to 7.2 with a mean estimate of M 6.8.

The minimum distance to earthquakes on the Stansbury fault ranges from 6.7 to 8.6 km, depending on the fault dip. The minimum distance to earthquakes on the postulated East Cedar Mountains fault ranges from 6.4 to 8.2 km, depending on the fault dip.

The application of 10 CFR Part 100 Appendix A to the assessment of maximum earthquakes includes the consideration of the potential for the maximum historical earthquake within the site tectonic province not associated with a specific seismic source to occur "near" the site. The term "near" has, by application, come to mean randomly within a 25-km radius of the site (Kimball, 1983). Most of the large earthquakes that have occurred in the Basin and Range province can be associated with specific faults. For this assessment, we have taken the conservative approach by assessing the maximum size of an earthquake that might occur on an unrecognizable fault. Because the hypothesized fault is unrecognized from surface geologic studies, its maximum magnitude is considered to be the largest earthquake that can occur without rupturing the surface (termed the threshold of surface faulting). Wells and Coppersmith (1993) have studied the presence or absence of surface faulting as a function of magnitude. Their studies have shown that the magnitude at which there is a 50% probability of surface faulting is magnitude 6; at magnitude 5.5 the probability is about 20% and at magnitude 6.5 the probability is about 80%. Based on these analyses, we consider the maximum magnitude for an earthquake occurring randomly in the site vicinity on an unknown source to be uniformly distributed in the range of M 5.5 to 6.5, with a mean value of 6.0. The earthquake location is assumed to be random within a 25-km radius circle. The resulting mean distance to the epicenter is 16.7 km. This event is smaller than those considered for the Stansbury fault.

4.2 Ground Motion Assessment

4.2.1 Approach

The ground motion assessments for the maximum earthquakes were made using empirical relationships that predict peak acceleration and response spectral accelerations as a function of earthquake magnitude, source-to-site distance, style of faulting, and generalized site classification. The empirical relationships provide estimates of the median ground motion level and the variability of individual recordings about that median, typically expressed as the

standard deviation of a lognormal distribution about the median value. The standard approach used to assess design ground motions from maximum events for nuclear facilities is to use the 84th percentile of the empirical distribution of peak motions. We have extended this approach to include the uncertainty in maximum magnitude, minimum source-to-site distance, and selecting appropriate attenuation relationship in the estimation of the 84th percentile ground motion levels. The formulation used is given by the relationship

$$P(Z > z) = \sum_m p(m_i) \cdot \sum_r p(r_j | m_i) \cdot \sum_A p(A_k) \cdot P(Z > z | m_i, r_j, A_k) \quad (4-1)$$

where $p(m_i)$ is the discrete probability density function for maximum magnitude; $p(r_j)$ is the discrete probability density function for minimum distance given a maximum magnitude; $p(A_k)$ is the discrete probability density (weight) assigned to a particular attenuation relationship; and $P(Z > z | m_i, r_j, A_k)$ is the probability that ground motion parameter Z exceeds level z given maximum magnitude m_i , minimum distance r_j , and attenuation relationship A_k . Equation (4-1) is solved iteratively for the value of z that results in $P(Z > z)$ equal to 0.8416 (plus one standard deviation of a normal distribution).

4.2.2 Ground Motion Attenuation Relationships

Two key considerations in the selection of attenuation relationships are the style of faulting/tectonic environment and the generalized site conditions. The site lies within an extensional tectonic environment that is characterized by normal faulting. A number of studies have shown that the predicted ground motions for strike-slip and normal-slip faulting events are comparable (and different from reverse-slip faulting) (e.g., Idriss, 1991; Sadigh and others, 1993, 1997). Recent work (Spudich and others, 1997) indicates that ground motions from extensional tectonic regime earthquakes are lower than those from compressional regime earthquakes. Therefore, we use a mixture of attenuation relationships that have been developed for strike-slip faulting earthquakes occurring in California and relationships for extensional stress regime earthquakes developed for the U.S. Department of Energy's planned nuclear repository at Yucca Mountain, Nevada.

Most empirical ground motion attenuation relationships are developed for two types of generalized site conditions, either "deep soil" (over 100 ft of soil over rock) or "rock" (less than 10 ft of soil over rock). The rock underlying recording sites in California typically is

highly weathered and fractured such that the average near surface velocity is on the order of 2,000 ft/sec, with lower values at the surface. This type of bedrock has become to be called "California" rock, or soft rock, to distinguish it from the very hard rock occurring near the surface in much of the eastern United States. The effect of different rock types on site ground motions is now recognized as an important issue in ground motion assessment.

The available data on the subsurface conditions at the site comes from shallow bore holes, seismic refraction surveys, and seismic reflection surveys. The shallow bore hole data (Stone & Webster, 1997) indicate that the site is underlain by about 30 ft of silts and clays, followed by about 25 ft of very dense sands, underlain by very hard silts to a maximum bore hole depth of 100 ft. The seismic reflection surveys (Geosphere Midwest, 1997) indicate that the depth to bedrock at the site is in the depth range of 400 to 800 ft. On the basis of the depth to rock (greater than 100 ft) and the general soil conditions (alluvial soils), one would classify the Skull Valley site as a deep soil site. However, the shallow refraction surveys (Geosphere Midwest, 1997) indicate that the shear wave velocities approach that of soft rock (about 2000 ft/sec at a depth of about 50 ft. Although these velocities are somewhat uncertain, they are generally consistent with the description of the soils as being very hard or very dense. Based on this data, the site profile may have characteristics that are near that of "California rock." Thus we have used both rock and deep soil attenuation relationships to predict 84th-percentile spectra.

Figure 4-4 compares the 84th-percentile peak horizontal acceleration (PGA) attenuation relationships used to estimate the site ground motions. Figure 4-5 compares the 84th-percentile horizontal acceleration response spectra predicted by the various relationships for the mean maximum magnitude of M 7 and the average minimum distance of 7.7 km. [Note that the attenuation relationship developed by Spudich and others (1997) uses minimum distance to the surface projection of the rupture. For the Skull Valley PFSF site this distance is 0 because the site lies above the fault plane.] We have used multiple attenuation relationships in the assessment to reflect the uncertainty in estimating near field ground motions from large earthquakes. The selected relationships represent the most recent work in evaluating empirical strong motion data. The relationships of Abrahamson and Silva (1997), Campbell (1997), and Sadigh and others (1993, 1997) provide estimates for both rock and deep soil. We have included two additional relationships. Idriss (1991) provides estimates of ground motion for rock sites. Spudich and others (1997) have updated the relationships of

Boore and others (1993, 1997) for extensional stress regimes. They present relationships for both soil and rock sites. We believe that the rock site relationships of Boore and others (1993, 1997) under estimate the ground motions on rock sites. Therefore, we have used only the deep soil relationships of Spudich and others (1997). Each of the four rock site relationships and the four soil site relationships were given equal weight.

Not all of the selected attenuation relationships for horizontal motions also have associated vertical motion relationships. For rock site conditions, the relationships of Abrahamson and Silva (1997), Campbell (1997) and Sadigh and others (1993) provide vertical estimates. For soil site conditions, only the relationships of Abrahamson and Silva (1997) and Campbell (1997) provide vertical motion estimates. The approach taken was to estimate horizontal and vertical spectra with the same subset of attenuation relationships and use these spectra to compute a ratio of vertical to horizontal motions. This ratio was then used to scale the horizontal spectra computed using the full set of horizontal relationships to produce the vertical 84th percentile spectra.

4.2.3 Recommended Response Spectra

Figure 4-6 shows the horizontal 84th percentile spectra computed for the three nearby sources (e.g., Stansbury fault, postulated East Cedar Mountains fault, and a random source) incorporating the uncertainty in maximum magnitude, source-to-site distance, and selection of attenuation relationships. These three sources are expected to produce larger motions at the site than any of the other faults in the surrounding region. The other faults have comparable maximum magnitudes but are at significantly greater distances. The Wasatch fault is likely to have a larger maximum magnitude, but it is located more than 80 km from the site and the resulting ground motions would be much lower than those shown on Figure 4-6. Among the three local sources, the Stansbury fault is the controlling ground motion source.

Figure 4-7 shows the horizontal and vertical response spectra for rock and deep soil sites for the Stansbury fault. The vertical response spectra were computed using the approach discussed above. The ratio of vertical to horizontal motions is below a value of 0.5 at periods longer than 0.5 seconds. For this study, we used a minimum vertical to horizontal motion ratio of 0.5. Also we used the envelope of the response spectra obtained directly from the subset of vertical attenuation relationships and the vertical spectra obtained by scaling the horizontal spectra. The spectral ordinates for deep soil and rock site conditions are listed in

Table 4-1. The peak horizontal ground accelerations are 0.67 g for both rock and deep soil site conditions. The peak vertical ground accelerations are 0.66 g for deep soil site conditions and 0.69 g for rock site conditions.

As indicated on Figure 4-7, the predicted rock site motions are larger at short spectral periods (high frequencies) and the predicted soil site motions are larger at long spectral periods (low frequencies). Because it is uncertain at this time whether the site behaves as a rock or a deep soil site we recommend that the preliminary design spectra for the site be conservatively taken as the envelope of the rock and soil site response spectra shown on Figure 4-7. These envelope spectra are plotted on Figure 4-8 and listed in Table 4-1.

TABLE 4-1
**STANSBURY 84TH-PERCENTILE SPECTRA
 HORIZONTAL SPECTRAL ACCELERATIONS (G)**

PERIOD	DEEP SOIL	ROCK	ENVELOPE
0.01 (PGA)	0.67	0.67	0.67
0.03	0.67	0.67	0.67
0.05	0.83	0.87	0.87
0.075	1.05	1.08	1.08
0.1	1.26	1.27	1.27
0.15	1.47	1.55	1.55
0.2	1.60	1.63	1.63
0.3	1.65	1.51	1.65
0.5	1.54	1.16	1.54
0.75	1.34	0.83	1.34
1	1.13	0.65	1.13
1.5	0.77	0.42	0.77
2	0.54	0.30	0.54
3	0.33	0.17	0.33
4	0.22	0.11	0.22

VERTICAL SPECTRAL ACCELERATIONS (G)

PERIOD	DEEP SOIL	ROCK	ENVELOPE
0.01 (PGA)	0.66	0.69	0.69
0.02	0.66	0.69	0.69
0.05	1.18	1.20	1.20
0.075	1.48	1.50	1.50
0.1	1.54	1.54	1.54
0.15	1.38	1.37	1.38
0.2	1.18	1.17	1.18
0.3	0.88	0.86	0.88
0.5	0.64	0.58	0.64
0.75	0.53	0.41	0.53
1	0.45	0.33	0.45
1.5	0.33	0.24	0.33
2	0.24	0.17	0.24
3	0.14	0.11	0.14
4	0.098	0.077	0.098

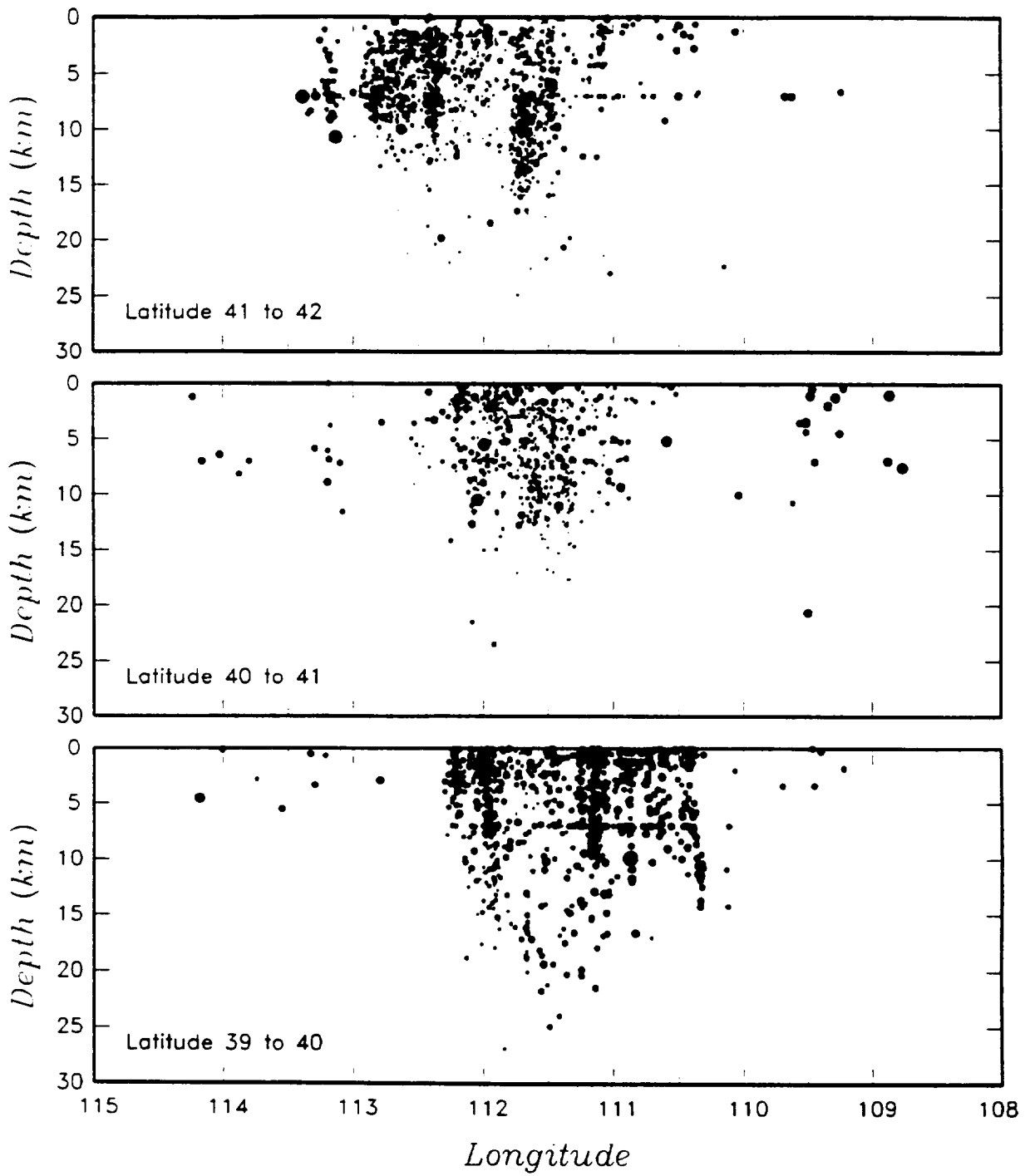


Figure 4-1 Seismicity cross sections along the Wasatch Front

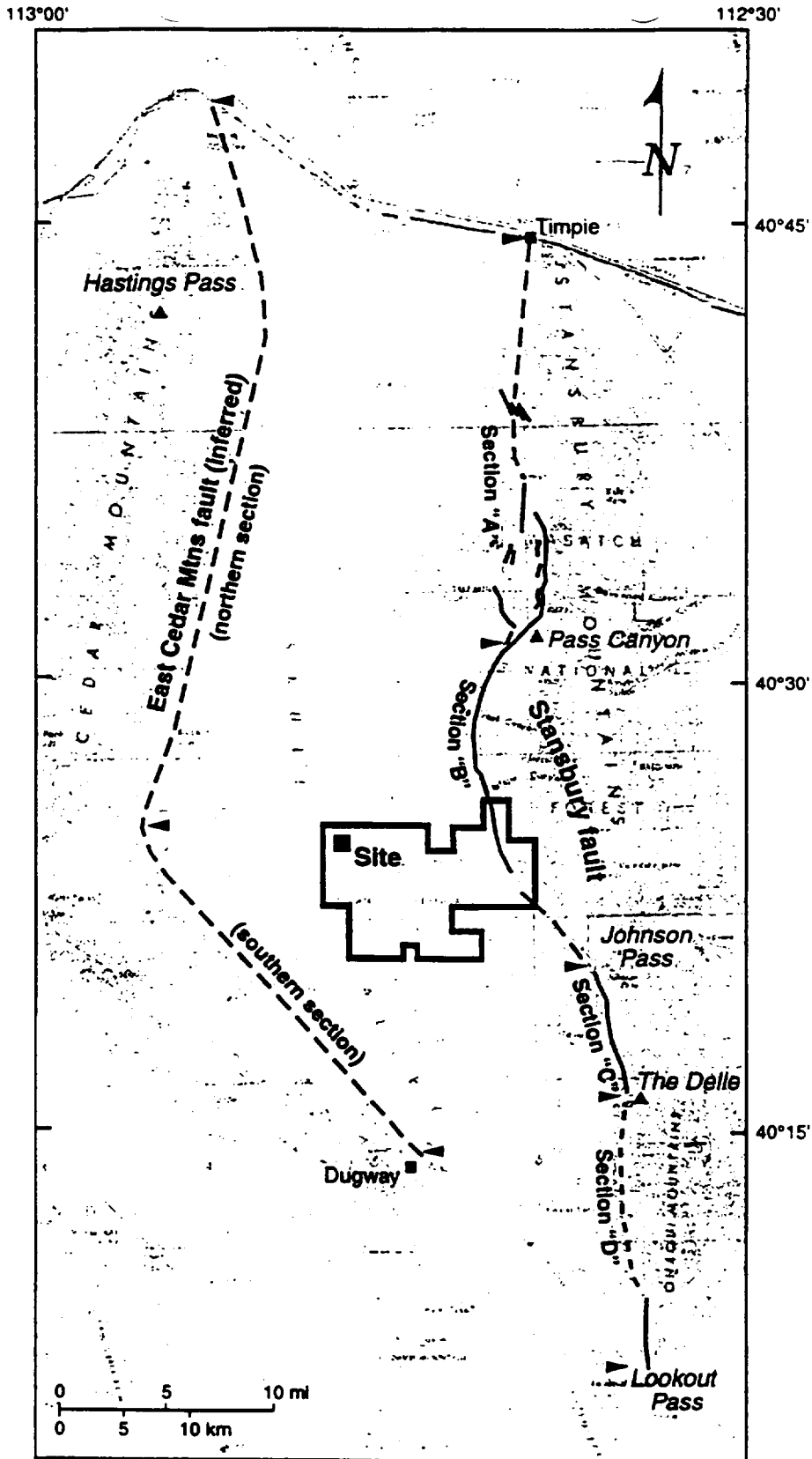


Figure 4-2 Sections of the Stansbury and East Cedar Mountains Faults. East Cedar Mountains fault after Hood and Waddell (1968); Stansbury fault after Helm (1995), Hecker (1993), and Sack (1993). Triangles show section ends.

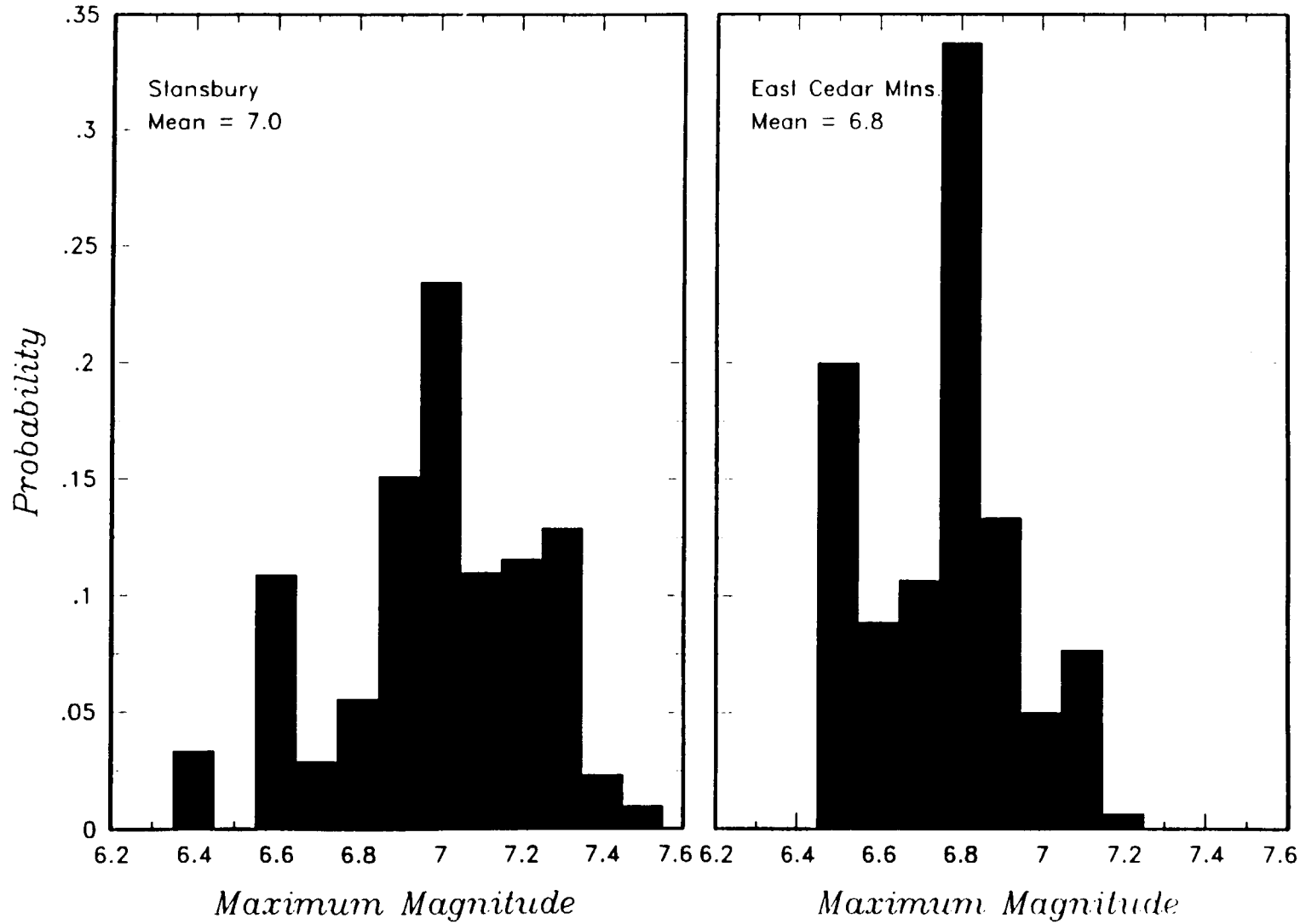


Figure 4-3 Maximum magnitude distributions for the Stansbury and East Cedar Mountains faults

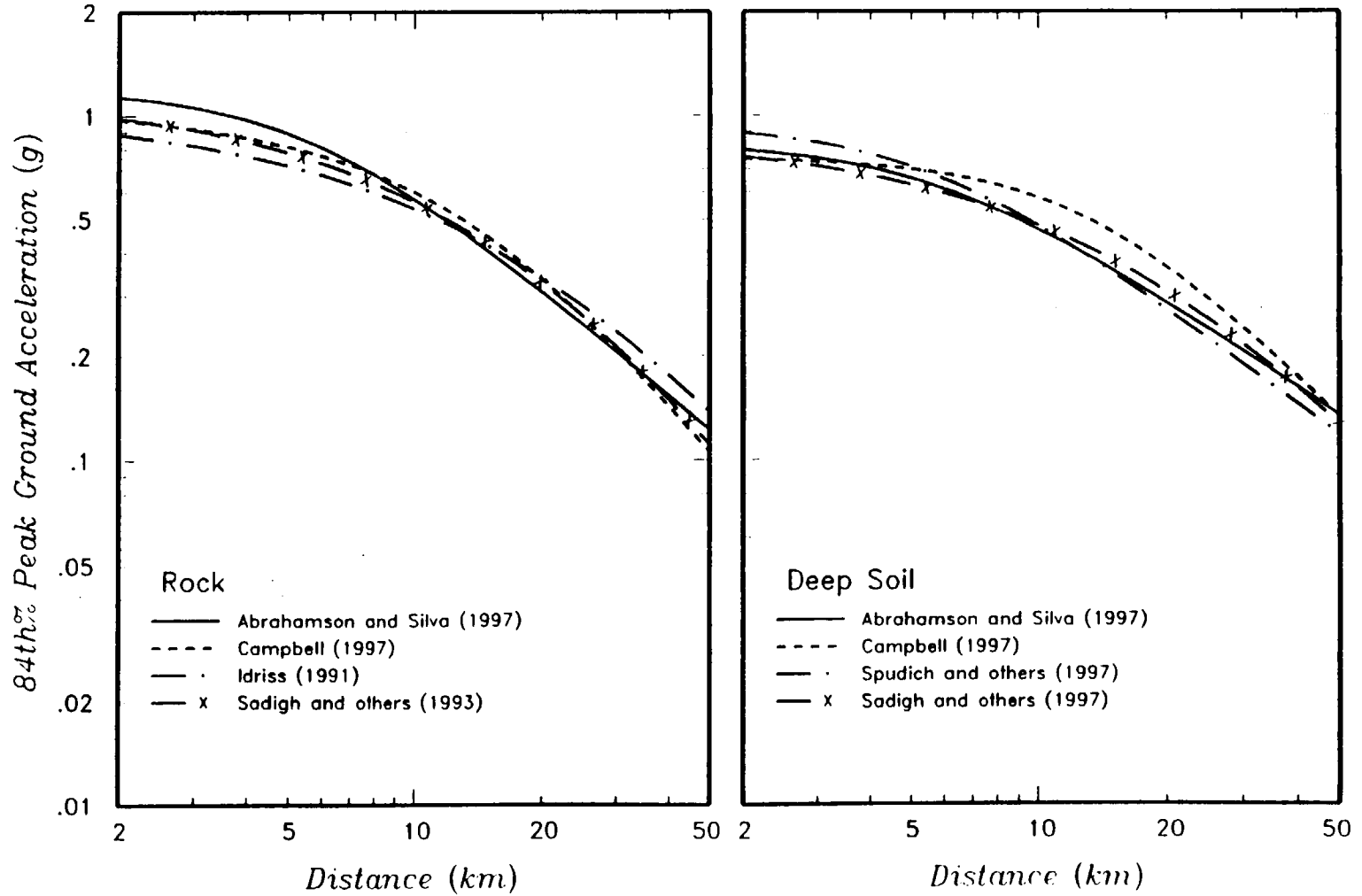


Figure 4-4 Comparison of horizontal PGA Attenuation Relationships

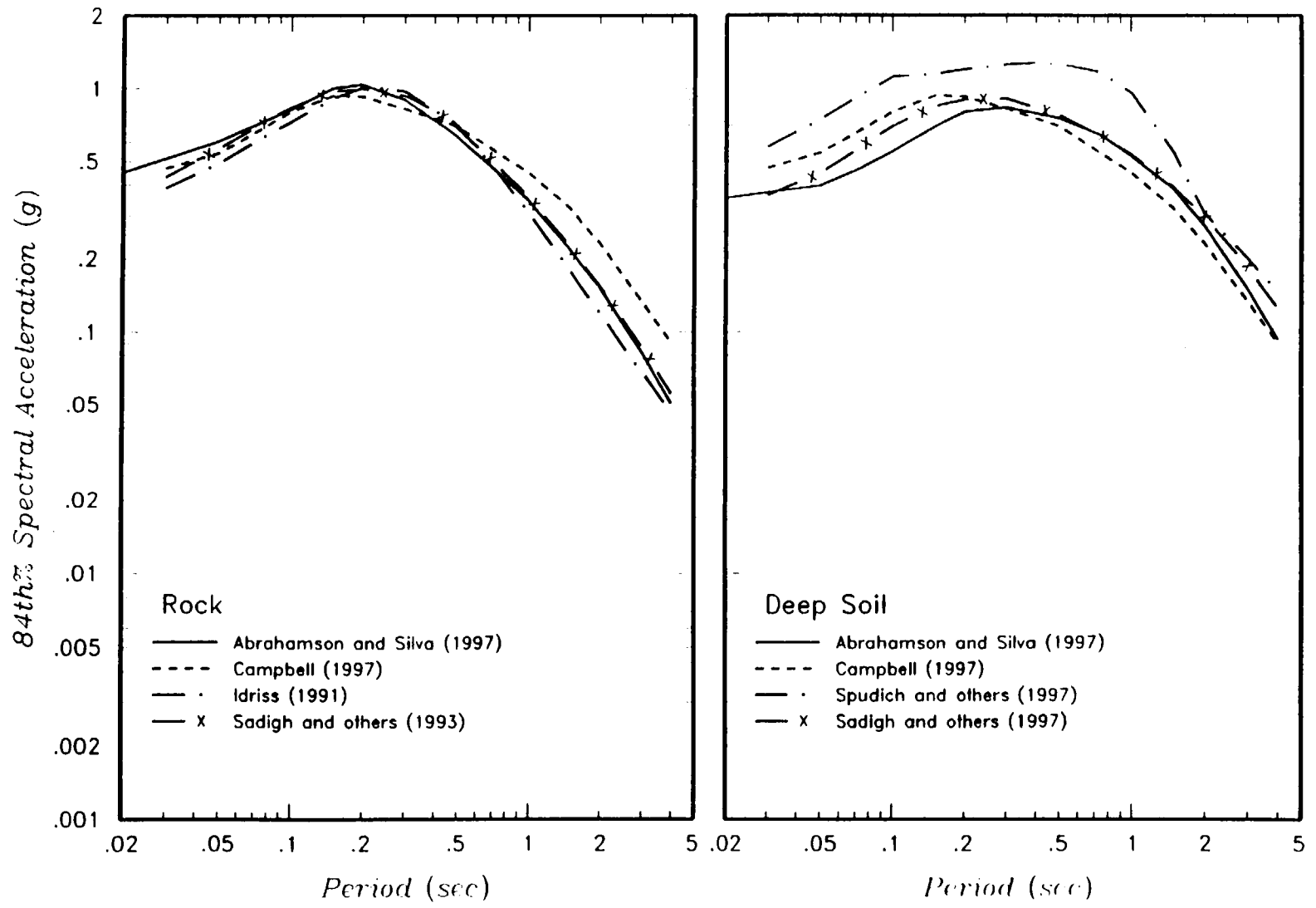


Figure 4-5 Comparison of horizontal acceleration response spectra

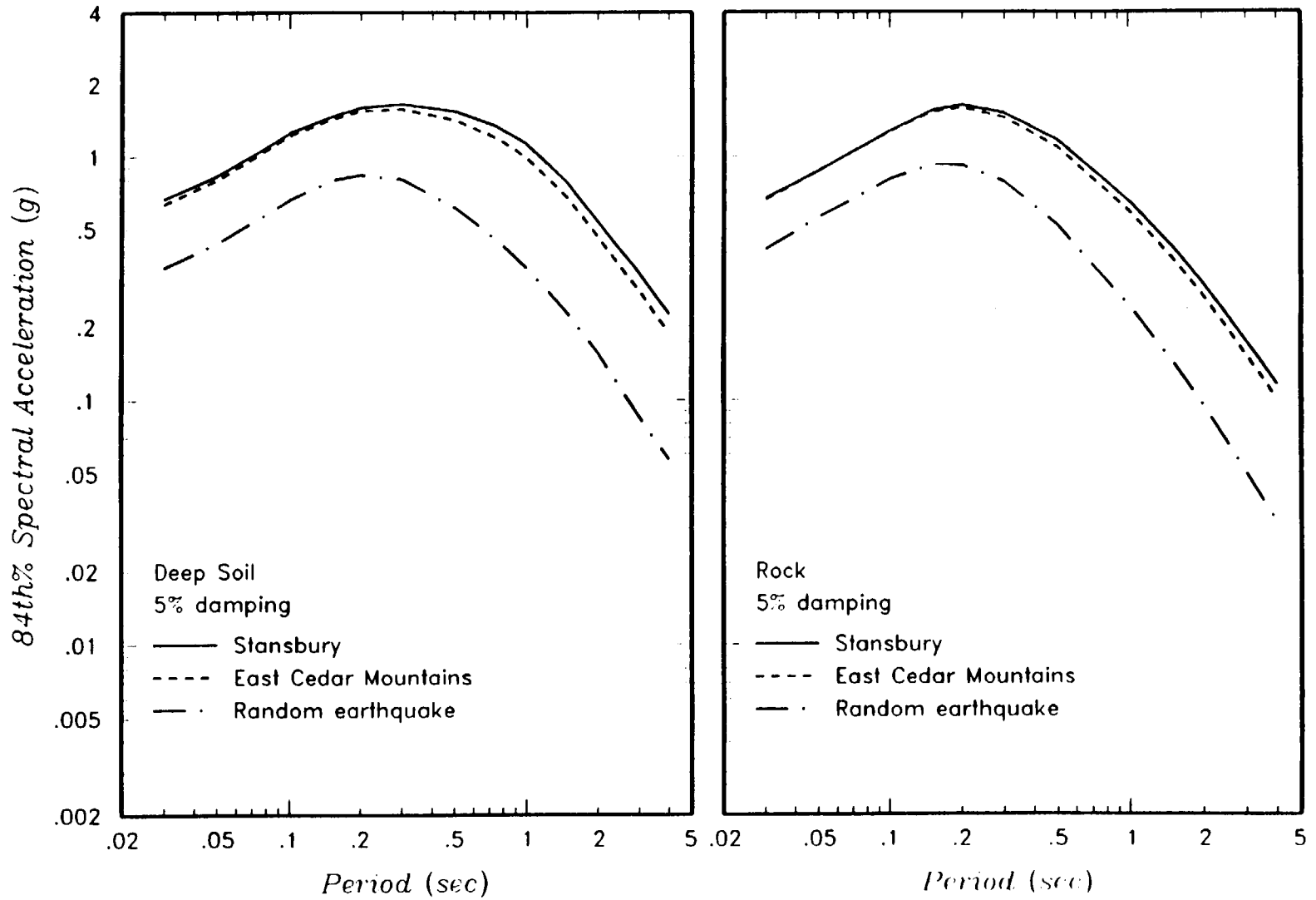


Figure 4-6 Comparison of 84th percentile horizontal response spectra for the three nearby seismic sources

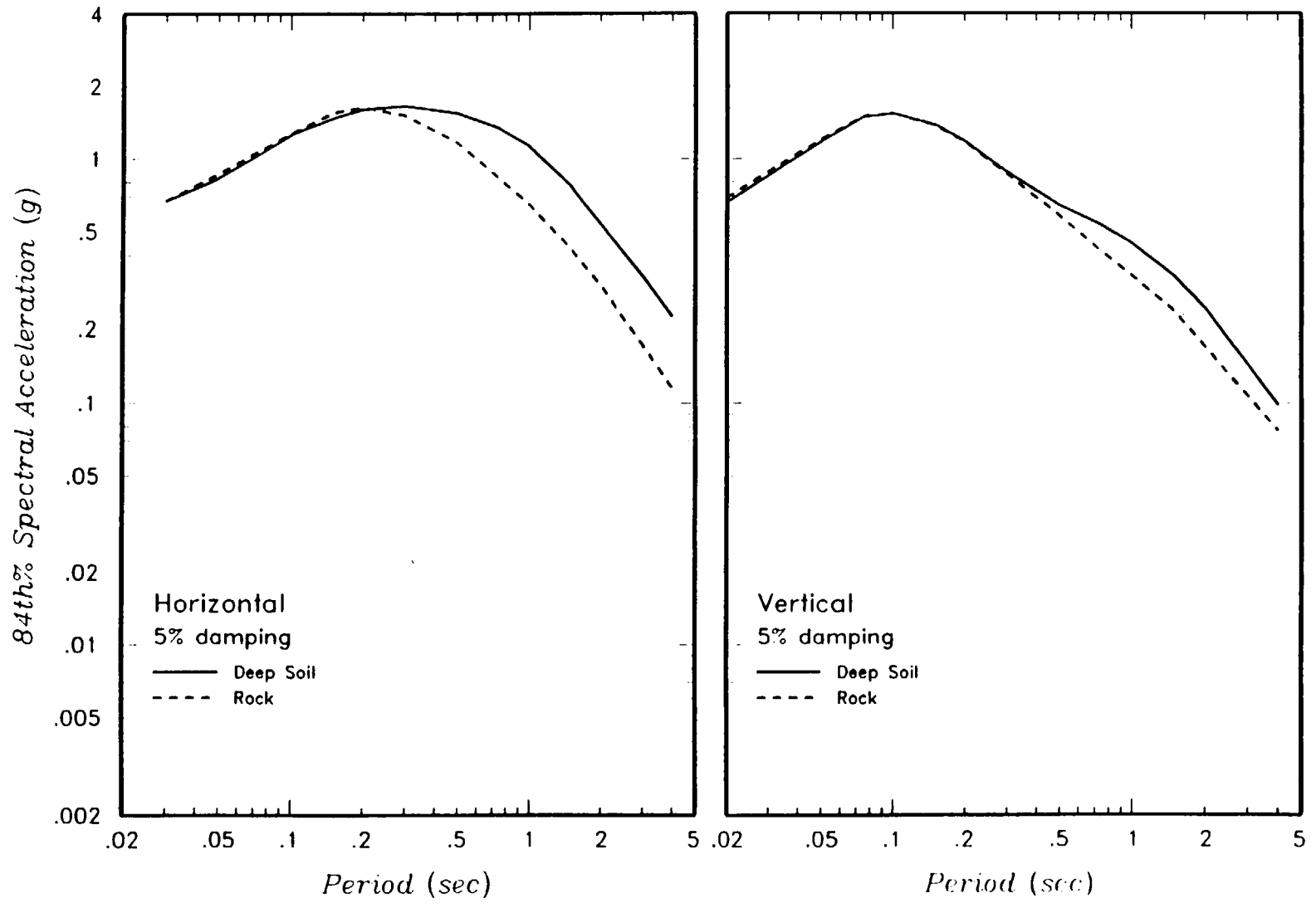


Figure 4-7 Stansbury fault 84th-percentile response spectra

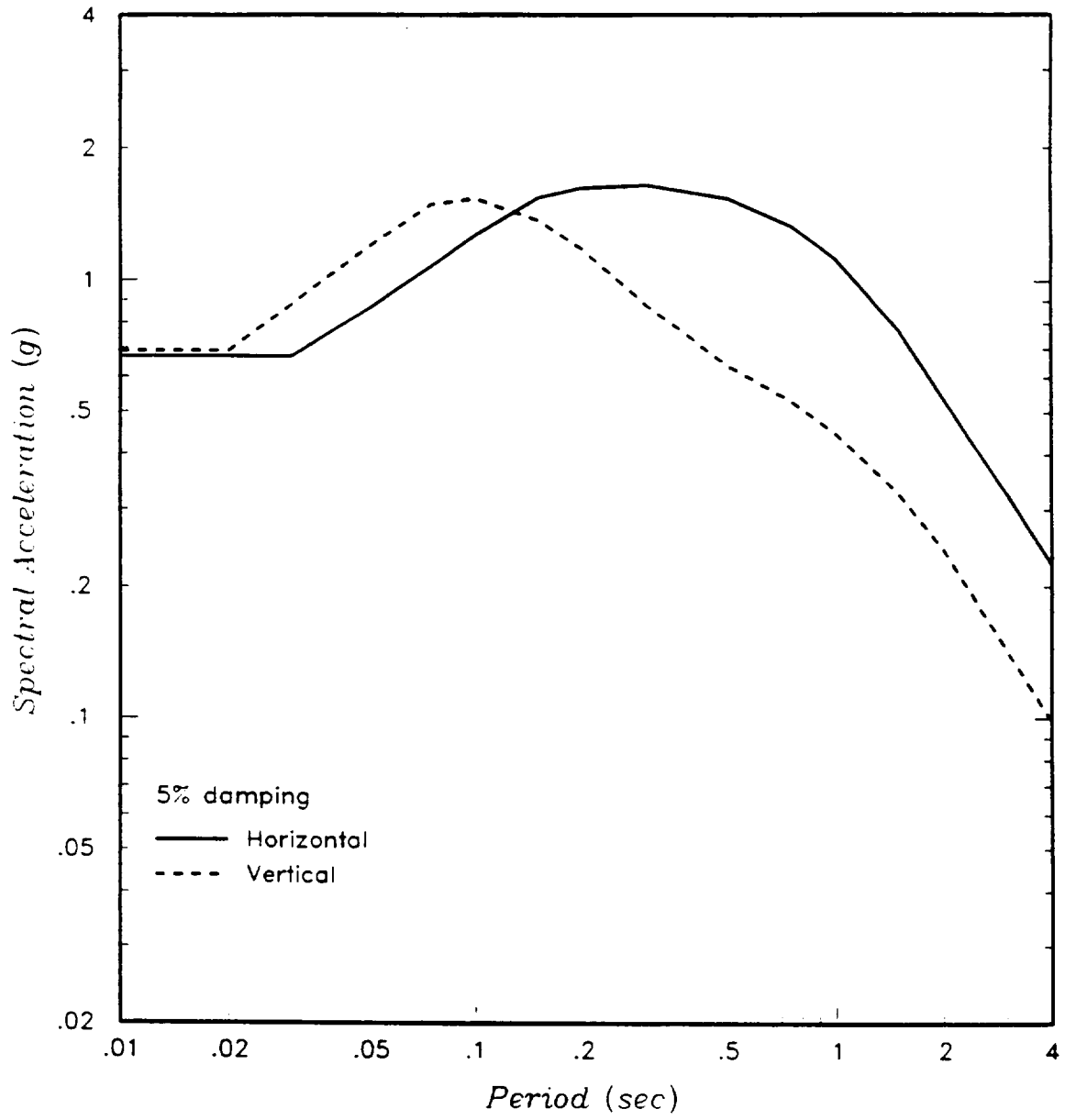


Figure 4-8 Recommended envelope 84th percentile response spectra

5.0 SUMMARY AND CONCLUSIONS

Using the methodologies that have been established for assessing ground motions for design of nuclear power plant facilities (e.g., Appendix A to 10 CFR100, and associated applications), we have developed a deterministic ground motion assessment for the PFSF site in Skull Valley, Utah. After evaluation of the seismotectonic setting and evaluation of potential seismogenic sources within the region, two capable or potentially capable fault sources are identified that lie within 10 km of the site. These are the Stansbury fault, which lies about 9.5 km to the east of the site, and a potential fault along the east side of the Cedar Mountains lying about 9 km to the west of the site. In addition, the potential for a “random nearby” earthquake (by convention lying within 25 km of the site) is also considered. Other capable faults lie more than 20 km from the site and are unlikely to produce 84th percentile ground motion levels that are as large as those estimated for the other sources.

Maximum magnitudes were estimated for each of the sources following common practice in western U.S. settings. No large historical earthquakes have occurred on any of the three sources that would be considered to be potential maximum events. Therefore, maximum rupture dimensions—rupture length and rupture area—were estimated for the two fault sources and empirical relationships used to arrive at moment magnitude estimates. The rupture length estimates incorporated evidence for segmentation of the fault zones and uncertainties in the length of coseismic ruptures. Likewise, uncertainties in the dip and downdip width of the faults was included in the assessment. The maximum magnitude distributions for the Stansbury and East Cedar Mountains faults are shown on Figure 4-3. The resulting mean estimates of maximum magnitude are **M 7.0** and **M 6.8** for the Stansbury and East Cedar Mountains faults, respectively.

The maximum magnitude associated with the random nearby source is estimated based on the conservative assumption that this earthquake will occur on an unrecognizable fault. Based on a consideration of the threshold of surface faulting, a maximum magnitude ranging from **M 5.5** to **M 6.5**, with a mean value of **6** is assessed for the zone. The earthquake location is assumed to be random within a 25-km radius circle, resulting in a mean distance to the epicenter of 16.7 km.

The ground motion assessments for the maximum earthquakes were made using empirical relationships that predict peak acceleration and response spectral accelerations as a function of earthquake magnitude, source-to-site distance, style of faulting, and generalized site classification. The standard approach used to assess design ground motions from maximum events for nuclear facilities is to use the 84th percentile of the empirical distribution of peak motions. We have extended this approach to include the uncertainty in maximum magnitude, minimum source-to-site distance, and selecting appropriate attenuation relationships in the estimation of the 84th percentile ground motions.

To account for the style of faulting, a mixture of attenuation relationships was used that have been developed for strike-slip faulting earthquakes occurring in California and relationships for extensional stress regime earthquakes. The available geophysical and geotechnical data for the site suggest that it may have the characteristics of either a “deep soil” site or may have the characteristics of a “California rock” site. Thus we have used both rock and deep soil attenuation relationships to predict 84th-percentile spectra. We have used multiple attenuation relationships in the assessment to reflect the uncertainty in estimating near field ground motions from large earthquakes.

Because there are few attenuation relationships for vertical motions, the approach taken was to estimate horizontal and vertical spectra with the same subset of attenuation relationships and use these spectra to compute a ratio of vertical to horizontal motions. This ratio was then used to scale the horizontal spectra computed using the full set of horizontal relationships to produce the vertical 84th percentile spectra.

Comparison of the ground motions for the three nearby sources shows that the Stansbury fault is the controlling ground motion source. Figure 4-7 shows the horizontal and vertical response spectra for rock and deep soil sites for the Stansbury fault. The peak horizontal ground accelerations are 0.67 g for both rock and deep soil site conditions. The peak vertical ground accelerations are 0.66 g for deep soil site conditions and 0.69 for rock site conditions. Because it is uncertain at this time whether the site behaves as a rock or a deep soil site, we recommend that the preliminary design spectra for the site be conservatively taken as the envelope of the response spectra shown in Figure 4-7. These envelope spectra are plotted on Figure 4-8 and listed in Table 4-1.

REFERENCES

- Abrahamson, N.A., and W.L. Silva, 1997, Empirical response spectral attenuation relations for shallow crustal earthquakes: *Seismological Research Letters*, v. 68, n. 1, p. 94-127.
- Anderson, J.G., Wesnousky, S.G., and Stirling, M.W., 1996, Earthquake size as a function of fault slip rate, *Bulletin of the Seismological Society of America*, v. 86, 3, p 683-690.
- Anderson, L.W., and Miller, D.G., 1979, Quaternary fault map of Utah: Long Beach, California, Fugro, Inc., 35 p., scale 1:500,000.
- Arabasz, W.J., Pechmann, J.C., and Brown, E.D., 1989, Evaluation of seismicity relevant to the proposed siting of a Superconducting Supercollider (SSC) in Tooele County, Utah: Utah Geological and Mineral Survey Miscellaneous Publication 89-1, 107 p.
- Barnhard, T.P., and Dodge, R.L., 1988, Map of fault scarps formed on unconsolidated sediments, Tooele 1° x 2° quadrangle, northwestern Utah: U. S. Geological Survey Miscellaneous Field Studies Map MF-1990, scale 1:250,000.
- Jack R. Benjamin and Associates, Inc., and Geomatrix, Inc., 1994, Probabilistic seismic hazard assessment for the U.S. Army Chemical Demilitarization Facility, Toole, Utah: unpublished consultant's report prepared for Science Applications International Corporation, Abington, Maryland.
- Boore, D.M., W.B. Joyner, and T.E. Fumal, 1993, Estimation of response spectra and peak acceleration from western North American earthquakes: an interim report: U.S. Geological Survey Open-File Report 93-509, 72 p.
- Boore, D.M., W.B. Joyner, and T.E. Fumal, 1997, Equations for estimating horizontal response spectra and peak acceleration from western North American earthquakes: a summary of recent work: *Seismological Research Letters*, v. 68, n. 1, p. 128-153.
- Brimhall, W.H., and Merritt, L.B., 1981, The geology of Utah Lake, implications for resource management: *Great Basin Naturalist Memoirs* Number 5, p. 24-42, scale 1:250,000.
- Bucknam, R.C., 1977, Map of suspected fault scarps in unconsolidated deposits, Tooele 1° x 2° sheet, Utah: U. S. Geological Survey Open-File Report 77-495.
- Bucknam, R.C., and Anderson, R.E., 1979, Map of fault scarps on unconsolidated sediments, Delta 1° x 2° quadrangle, Utah: U.S. Geological Survey Open-File Report 79-366, 21 p., scale 1:250,000.

- CH2M Hill, Inc., 1986. Geologic field analysis for siting a chemical agent stockpile disposal system at the Tooele Army Depot, South Area. Tooele County, Utah: unpublished report prepared for the U.S. Army Engineering Division, Huntsville, Alabama.
- Campbell, K.W., 1997, Empirical near-source attenuation relationships for horizontal and vertical components of peak ground acceleration, peak ground velocity, and pseudo-absolute acceleration response spectra: *Seismological Research Letters*, v. 68, n. 1, p. 154-179.
- Christiansen, R.L., and Yeats, R.S., 1992, Post-Laramide geology of the U.S. Cordilleran region: in Burchfield, B.C., Lipman, P.W., and Zoback, M.L. (eds.), *The Cordilleran Orogen: Conterminous U.S.: Geological Society of America, The Geology of North America*, v. G-3, p. 261-406.
- Cook, K.L., Gray, E.F., Iverson, R.M., and Strohmeier, M.T., 1980, Bottom gravity meter regional survey of the Great Salt Lake, Utah: in Gwynn, J.W. (ed.), *Great Salt Lake, a scientific, historical and economic overview: Utah Geological and Mineralogical Survey Bulletin 116*, p. 125-143.
- Currey, D.C., 1996, Final Report of a geomorphological survey of surficial lineaments north of Hickman Knolls, Tooele County, Utah: prepared by Limnetectonics Laboratory for Stone & Webster Engineering Corporation, 4 pp.
- Currey, D.R., Atwood, G., and D.R. Mabey, 1983, Major levels of Great Salt Lake and Lake Bonneville; *Utah Geological Survey Map 73*, 1:750,000-scale plate.
- dePolo, C.M., Clark, D.G., Slemmons, D.B., and Aymard, W.H., 1989, Historical Basin and Range Province surface faulting and fault segmentation: in Schwartz, D.P., and Sibson, R.H. (eds.), *Fault segmentation and controls of rupture initiation and termination — proceedings of conference XLV: U. S. Geological Survey Open-File Report 89-315*, p. 131-162.
- Dixon, T.H., Robaudo, S., Lee, J., and Reheis, M.C., 1995, Constraints on present-day Basin and Range deformation from space geodesy: *Tectonics*, v. 14, p. 755-772.
- Doser, D.I., 1989, Extensional tectonics in northern Utah-southern Idaho, USA, and the 1934 Hansel Valley sequence: *Physics of the Earth and Planetary Interiors*, v. 54, no.1-2, p. 120-134.
- Eddington, P.K., Smith, R.B., Renggli, C., 1987, Kinematics of Basin and Range intraplate extension: in Coward, M.P., Dewey, J.F., and Hancock, P.L. (eds.), *Continental Extensional Tectonics: Geological Society of London Special Publication 28*, p. 371-392.

- England, P., and Jackson, J., 1989, Active deformation of the continents: *Annual Reviews of Earth and Planetary Science*, v. 17, p. 197-226.
- Everitt, B.L., and Kaliser, B.N., 1980, *Geology for assessment of seismic risk in the Tooele and Rush Valleys, Tooele County, Utah*: Utah Geological Survey Special Studies 51, 33 p.
- Ertec Western, Inc., 1981, MX siting investigation, faults and lineaments in the MX siting region, Nevada and Utah: Long Beach, California, unpublished consultant's report no. E-TR-54 for U. S. Air Force; volume I, 77 p.; volume II, variously paginated.
- Geosphere Midwest, 1997, *Seismic survey of the Private Fuel Storage Facility, Skull Valley, Utah*: report prepared for Stone & Webster Engineering Corporation
- Hanks, T.C., Buchnam, R.C., Jajoie, K.R., and Wallace, R.E., 1984, Modifications of wave-cut and faulting-controlled landforms: *Journal of Geophysical Research*, v. 89, no. B7, p. 5771-5790.
- Hecker, S., 1993, *Quaternary tectonics of Utah with emphasis on earthquake-hazard characterization*: Utah Geological Survey Bulletin 127, 157 p., 2 plates.
- Helm, J.M., 1995, *Quaternary faulting in the Stansbury fault zone, Toole County, Utah*: in W.R. Lund (ed.), *Environmental and Engineering Geology of the Wasatch Front Region*, Utah Geological Association Publication 24, p. 31-44.
- Hood, J. W., and K.M. Waddell, 1968, *Hydrologic reconnaissance of Skull Valley, Tooele County, Utah*: Utah Dept. Nat. Resour., Tech. Publ. No. 18, 57 p.
- Idriss, I.M., 1991, *Selection of earthquake ground motions at rock sites*: Report prepared for the Structures Division, Building and Fire Research Laboratory, National Institute of Standards and Technology, Department of Civil Engineering, University of California, Davis, September, updated in a 1993 memo.
- Jacobs Engineering Group, URS, and John A. Blume & Associates, 1988, *Geological-seismological investigation of earthquake hazards for a chemical agent demilitarization facility at the Toole Army Depot, Utah*: Prepared for the Office of the Program Manager for Chemical Munitions by U.S. Army Engineer Division, Huntsville, Alabama; Contract No. DACA87-86-0085, Delivery Order 0004, 114 p. plus appendices and figures.
- Jones, C.H., Unruh, J.R., and Sonder, L.J., *The role of gravitational potential energy in active deformation in the southwestern United States*: *Nature*, v. 381, no. 6577, p. 37-41.

- Keaton, J.R., Currey, D.R., and Olig, S.J., 1987, Paleoseismicity and earthquake hazards evaluation of the West Valley fault zone. Salt Lake City, Dames and Moore. Final Technical Report for U. S Geological Survey, Contract No. 14-08-0001-22048. 55 p.
- Kimball, J.K., 1983, The use of site dependent spectra: Proceedings of the U.S. Geological Survey Workshop on Site Specific Effects of Soil and Rock on Ground Motions and the Implications for Earthquake-Resistant Design, U.S. Geological Survey Open File Report 83-845. p. 401-422.
- Krinitzky, E.L., 1989, Empirical earthquake ground motions for an engineering site with fault sources—Tooele Army Depot, Utah: Bulletin of the Association of Engineering Geologists, v. 26, no. 3, p. 283-308.
- Machette, M.N., 1989, Preliminary surficial geologic map of the Wasatch fault zone, eastern part of Utah Valley, Utah County, and parts of Salt Lake and Juab Counties, Utah: U.S. Geological Survey Miscellaneous Field Studies Map MF-2109, scale 1:50,000.
- Machette, M.N., Personius, S.F., Nelson, A.R., Schwartz, D.P., and Lund, W.R., 1991, The Wasatch fault zone, Utah—segmentation and history of Holocene earthquakes: Journal of Structural Geology, v. 13, p. 137-149.
- Machette, M.N., Personius, S.F., and Nelson, A.R., 1992, Paleoseismology of the Wasatch fault zone, a summary of recent investigations, interpretation, and conclusion: in Gori, P.L. and Hays, W.W. (eds.), Assessment of regional earthquake hazards and risk along the Wasatch Front, Utah: U.S. Geological Survey Professional Paper 1500-A, 71 p.
- Malde, H.E., 1991, Quaternary geology and structural history of the Snake River Plain, Idaho and Oregon: in Morrison, R.B. (ed.), Quaternary nonglacial geology; Coterminal U.S.: Geological Society of America, The Geology of North America, v. K-2, p. 251-281.
- McCalpin, J.P., and Forman, S.L., 1991, Late Quaternary faulting and thermoluminescence dating of the East Cache fault zone, north-central Utah: Bulletin of the Seismological Society of America, v. 81, no. 1, p. 139-161.
- McCalpin, J.P., Robison, R.M., and Garr, J.D., 1992, Neotectonics of the Hansel Valley-Pocatello Valley corridor, northern Utah and southern Idaho: in Gori, P.L., and Hays, W.W. (eds.), Assessment of regional earthquake hazards and risk along the Wasatch Front, Utah: U.S. Geological Survey Professional Paper 1500-G, 18 p.

- Molnar, P., and Lyon-Caen, H., 1988. Some simple physical aspects of the support, structure, and evolution of mountain belts: in Clark, S.P., Burchfiel, B.C., and Suppe, J. (eds.), Processes in Continental Lithospheric Deformation: Geological Society of America Special Paper 218, p. 179-207.
- Moore, W.J., and Sorensen, M.L., 1979. Geologic map of the Tooele 1° x 2° quadrangle, Utah: U.S. Geological Survey Miscellaneous Investigations Series Map I-1132, scale 1:250,000.
- Morris, H.T., 1987. Preliminary geologic map of the Delta 2° quadrangle, Tooele, Juab, Millard, and Utah Counties, Utah: U.S. Geological Survey Open-File Report 87-185, 18 p., scale 1:250,000.
- Mukulich, M., and Smith, R.B., 1974. Seismic reflection and aeromagnetic surveys of the Great Salt Lake, Utah: Geological Society of America Bulletin, v. 85, p. 991-1002.
- Oldow, J.S., Bally, A.W., Ave` Lallemand, H.G., and Leeman, W.P., 1989. Phanerozoic evolution of the North American Cordillera; United States and Canada: in Bally, A.W., and Palmer, A.R. (eds.), The Geology of North America-An Overview: The Geology of North America, v.A, Geological Society of America, Boulder, Colorado, p. 139-232.
- Olig, S.S., Lund, W.R., and Black, B.D., 1995. Large mid-Holocene and late Pleistocene earthquakes on the Oquirrh fault zone, Utah: Geomorphology, v. 10, p. 285-315.
- Pechmann, J.C., Nash, W.P., Viveiros, J.J., and Smith, R.B., 1987. Slip rate and earthquake potential of the East Great Salt Lake fault, Utah (abs.): EOS Transactions, American Geophysical Union, v. 68, p. 1369.
- Pierce, K.L., and Colman, S.M., 1986. Effect of height and orientation (microclimate) on geomorphic degradation rates and processes, late glacial terrace scarps in central Idaho: Geological Society of America Bulletin, v. 97, no. 7, p. 869-885.
- Rigby, J.K., 1958. Geology of the Stansbury Mountains, Toole County, Utah: Utah Geological Society Guidebook 13, 168 p.
- Rogers, A.M., Harmsen, S.C., Corbett, E.J., Priestley, K., and dePolo, D., 1991. The seismicity of Nevada and some adjacent parts of the Great Basin: in Slemmons, D.B., Engdahl, E.R., Zoback, M.D., and Blackwell, D.D. (eds.), Neotectonics of North America: Geological Society of America Decade Map Volume 1, p. 153-184.
- Rowley, P.D., Anderson, J.J., Williams, P.L., and Fleck, R.J., 1978. The age of structural differentiation between the Colorado Plateau and Basin and Range provinces in southwestern Utah: Geology, v. 6, p. 51-55.

- Sack, D., 1993, Quaternary geologic map of Skull Valley, Tooele County, Utah: Utah Geological Survey Map 150, scale 1:100,000.
- Sadigh, K., Chang, C.-Y., Abrahamson, N.A., Chiou, S.J., and Power, M.S., 1993. Specification of long-period ground motions: updated attenuation relationships for rock site conditions and adjustment factors for near-fault effects: Proceedings of ATC-17-1 Seminar on Seismic Isolation, Passive Energy Dissipation, and Active Control, March 11-12, San Francisco, California, p. 59-70.
- Sadigh, K., Chang, C.-Y., Egan, J.A., Makdisi, F., and Youngs, R.R., 1997, Attenuation relationships for shallow crustal earthquakes based on California strong motion data: Seismological Research Letters, v. 68, n. 1, p. 154-179.
- Sibson, R.H., 1982, Fault zone models, heat flow, and the depth distribution of earthquakes in the continental crust of the United States: Bulletin of the Seismological Society of America, v. 72, p. 151-163.
- Sibson, R.H., 1984, Roughness at the base of the seismogenic zone—contributing factors: Journal of Geophysical Research, v. 89, p. 5791-5799.
- Smith, R.B., and Arabasz, W.J., 1991, Seismicity of the intermountain seismic belt: in Slemmons, D.B., Engdahl, E.R., Zoback, M.D., and Blackwell, D.D. (eds.), Neotectonics of North America: Boulder, Colorado, Geological Society of America, Decade Map Vol. 1.
- Smith, R.B., and Bruhn, R.L., 1984, Intraplate extensional tectonics of the eastern Basin-Range; inferences on structural style from seismic reflection data, regional tectonics, and thermal-mechanical models of brittle/ductile deformation: Journal of Geophysical Research, v. 89, p. 5733-5762.
- Smith, R.B., Richins, W.D., and Doser, D.I., 1985, The 1983 Borah Peak, Idaho earthquake - regional seismicity, kinematics of faulting, and tectonic mechanism: Proceedings of Workshop XXVIII on the Borah Peak, Idaho, Earthquake, v. A, U.S. Geological Survey Open-File Report 85-290, p. 236-263.
- Solomon, B.J., 1993, Quaternary geologic maps of Tooele Valley and the West Desert Hazardous Industry Area, Tooele County, Utah: Utah Geological Survey Open-File Report 296, 48 p. 1:24,000 scale.

- Spudich, P. Fletcher, J.B., Hellweg, M., Boatwright, J., Sullivan, C., Joyner, W.B., Hanks, T.C., Boore, D.M., McGarr, A., Baker, L.M., and Lindh, A.G., SEA96 - a new predictive relation for earthquake ground motions in extensional tectonic regimes: *Seismological Research Letters*, v. 68, n. 1, p. 190-198.
- Stone & Webster Engineering Corporation, 1997, Geotechnical Data Report No. 05996.01-G(B)-Z Rev 0.
- Sullivan, J.T., Meeder, C.A., Martin, R.A., and West, M.W., 1980. Seismic hazard evaluation of Ridgway dam and reservoir site, Dallas Creek Project, Colorado: Seismotectonic section, Geologic Services Branch, Division of Geology, U.S. Water and Power Resources Service, Denver, Colorado, 44 p. plus appendices.
- Viveiros, J.J., 1986, Cenozoic tectonics of the Great Salt Lake from seismic reflection data: M.S. thesis, University of Utah, Salt Lake City, Utah, 81 p.
- Wells, D. W., and K. J. Coppersmith, 1994, New empirical relationships among magnitude, rupture length, rupture width, rupture area, and surface displacement, *Bulletin of the Seismological Society of America*, v. 84, p. 974-1002.
- Wernicke, B., 1992, Cenozoic extensional tectonics of the U.S. Cordillera: in Burchfiel, B.C., Lipman, P.W., and Zoback, M.L. (eds.), *The Cordilleran Orogen: Conterminous U.S.:* Geological Society of America, *The Geology of North America*, v. G-3, p. 553-581.
- Wong, I.G., and Humphrey, J.R., 1989. Contemporary seismicity, faulting and the state of stress in the Colorado Plateau: *Geological Society of America Bulletin*, v. 101, p. 1127-1146.
- Wyss, M., 1979, Estimating maximum expectable magnitude of earthquakes from fault dimensions: *Geology*, v. 7, p. 336-340.
- Young, J. C., 1955, *Geology of the southern Lakeside Mountains, Utah:* Utah Geological and Mineral Survey Bulletin 56, 116 p.
- Youngs, R.R., Swan, F.H., III, Power, M.P., Schwartz, D. P., and Green, R.K., 1987, Analysis of earthquake ground shaking hazard along the Wasatch Front, Utah: in Gori, P.L., and Hays, W.W. (eds.), *Assessment of regional earthquake hazards and risk along the Wasatch Front, Utah, volume II:* U.S. Geological Survey Open-File Report 87-585, p. M-1-110.

Zoback, M.L., and Zoback, M.D., 1989. Tectonic stress field of the continental United States:
in Pakiser, L.C., and Mooney, W.D. (eds.). Geophysical Framework of the Continental
United States: Geological Society of America Memoir 172, p. 523-540.

OBJECTIVE

Set forth PFS's justification for a 1,000 year seismic recurrence interval used in establishing the design basis ground motion at the PFSF site, based on relative risk.

RADIOLOGICAL CONSEQUENCES OF EARTHQUAKES AT THE PFSF

Both the HI-STORM and TranStor storage casks were analyzed for cask stability for the original PFSF site specific design earthquake, calculated using the deterministic methodology of 10 CFR 100 Appendix A. This earthquake was characterized by response spectrum curves developed specifically for the site with zero period accelerations of 0.67g horizontal (two directions) and 0.69g vertical. The response spectrum curves for the PFSF original site specific deterministic design earthquake are documented in Reference 1 (previously PFSF SAR Appendix 2D). Recent highly detailed seismological studies have found additional faulting in the vicinity of the PFSF site (Reference 2).

Accounting for these faults in the deterministic seismic hazard analysis results in peak ground acceleration values slightly higher (approximately 10%) than those identified for the original deterministic design earthquake. The cask stability analysis for the original PFSF site specific design earthquake (zero period accelerations of 0.67g horizontal and 0.69g vertical) determined the response of the storage casks to the earthquake accounting for soil-structure interaction, with the soil parameters and design of the concrete storage pads specific to the PFSF. The analysis concluded that while the casks would not remain stationary but could slide, rock and rim, movements were sufficiently small as to prevent any cask collisions, cask tipover, or sliding of casks off the storage pads. It was determined that the canisters would be subjected to relatively small stresses and their integrity was not challenged, so no release of radioactivity would occur.

The response spectrum of the PFSF original deterministically derived site specific design earthquake bounds that associated with the current design basis ground motion calculated by a probabilistic seismic hazard analysis using a 1,000 year recurrence interval (0.40g horizontal and 0.39g vertical peak ground accelerations).

The bounding consequences of a major seismic event at the PFSF using the HI-STORM and TranStor systems technology are defined by a storage cask tipover event, although this would only occur at ground motions well above those associated with the original PFSF site specific design earthquake for which the storage casks have been analyzed. While cask tipover is not a credible event, the canisters are designed to withstand the stresses resulting from a non-mechanistic cask tipover event with no breach and no release of radioactive material from inside the canister.

The canisters for both the the HI-STORM and TranStor storage systems are multi-purpose canisters designed for conditions of transport and storage. The transport system is required by 10 CFR 71.73 to be demonstrated capable of

withstanding a 30 ft drop. Both vendors have designed the canisters to withstand stresses resulting from this event. The design basis loadings of these canisters are 45g's for the HI-STORM canister and 44g's for the TranStor canister. As demonstrated in the vendors' storage system SARs, accelerations resulting from hypothetical storage cask tipover are below these design accelerations, and resultant canister stresses are within allowables. Canisters would retain their integrity in the event of storage cask tipover.

Spent fuel rod cladding will not breach as the result of a seismic event at the PFSF, even if the event were of a magnitude well beyond the seismic design basis such that it resulted in a storage cask tipover. For example, Section 3.5 of the HI-STORM SAR states:

“Studies of the capability of spent fuel rods to resist impact loads [3.5.1] indicate that the most vulnerable fuel can withstand 63g's in the most adverse orientation. Therefore, designing the HI-STORM 100 System to a maximum deceleration of 45g's will ensure that fuel rod cladding integrity is maintained during all normal, off-normal, and accident conditions.”

Both the HI- STORM and TranStor canisters are demonstrated to maintain their integrity in the event of a hypothetical storage cask tipover event. Since a cask tipover represents the worst-case effects of a seismic event whose magnitude exceeds the design basis, there are no radiological consequences associated with seismic events.

RELATIVE RISK ASSOCIATED WITH EARTHQUAKES AT THE PFSF, AND DETERMINATION OF SEISMIC RECURRENCE INTERVAL

Risk is defined as the probability of occurrence of an event times the consequences associated with that event. The consequences of interest are radiological doses to members of the general public. Since there are no radiological consequences of seismic events, as discussed above, an earthquake produces negligible radiological risk.

Although there are no radiological consequences resulting from a seismic event, the PFS seismic exemption request considered radiological consequences that are associated with other accidents analyzed for the facility in order to incorporate a conservative margin of safety. The accident that has the greatest radiological consequences is canister leakage under hypothetical accident conditions in which 100% of the fuel rod cladding in the leaking canister is assumed to have breached (SAR Section 8.2.7). PFS compared dose consequences of this hypothetical accident with NRC staff guidelines developed for seismic events.

An approach similar to PFS's was taken for the TMI-2 ISFSI seismic analysis. In SECY-98-071 (Reference 3), the NRC staff states:

"In reviewing DOE-ID's exemption request, the staff considered foremost the public health and safety consequences of a major seismic event at a cask or canister ISFSI. At an ISFSI using the NUHOMS system technology, the consequences are bounded by a canister drop onto the concrete pad. Although this would occur only at a ground motion well above the proposed design earthquake of 0.36g peak ground acceleration, the canisters are designed to withstand such drops with no release of radioactive material. DOE-ID estimates that should a storage canister fall and one of the 12 inner core debris canisters release its contents (although the staff has not identified a credible mechanism for such a failure), the radiological consequences would be a dose of about 0.75 mSv (75 mrem) to a member of the public."

Radiological consequences of the PFSF canister leakage under hypothetical accident conditions were determined to be approximately 75 mrem total effective dose equivalent (TEDE) for a postulated leaking TranStor canister containing BWR spent fuel, which produced higher doses than a leaking TranStor canister containing PWR spent fuel and HI-STORM canisters containing either PWR or BWR spent fuel, as discussed in PFSF SAR Section 8.2.7. This accident involved failure of a SSC important to safety in which a canister is postulated to leak for 30 days under hypothetical accident conditions with 100% of the fuel rod cladding assumed to have failed, analyzed in accordance with the NRC's Interim Staff Guidance-5. The analysis conservatively assumed that the exposed individual was continuously located at the PFSF owner controlled area boundary for the 30 days leak duration, with the wind constantly blowing in this direction under severe meteorological conditions.

Although this worst-case PFSF accident is unrelated to a seismic event, the consequences were nonetheless compared to the criteria relating accident dose consequences to seismic recurrence intervals set forth in NRC documents. In SECY-98-126 (Reference 4), concerning the NRC's rulemaking for geological and seismological characteristics for siting and design of dry cask ISFSIs under 10 CFR 72, the NRC staff states under Option 3, its preferred option for amending Part 72, the following related to the Part 60 design basis event rulemaking:

"The specific approach proposed for dry cask ISFSI systems, structures, and components would be comparable to the 10 CFR Part 60 graded approach to design ground motion for SSCs of pre-closure facilities. This graded approach would allow the structures, systems, and components of dry cask ISFSIs to be designed to either Frequency-Category-1 design basis events or Frequency-Category-2 design basis events, depending upon their importance-to-safety. For seismic events, the staff has accepted the approach described in DOE Topical Report YMP/TR-003-NP, Rev. 2, Preclosure Seismic Design Methodology for a Geologic Repository at Yucca Mountain, pertaining to 10 CFR Part 60. In this approach, Frequency-Category-1 design basis ground motion refers to a mean annual probability of

exceedance of $1.0E-03$, which corresponds to a 1,000-year return period. Frequency-Category-2 design basis ground motion refers to a mean annual probability of exceedance of $1.0E-04$, which corresponds to a 10,000-year return period."

10 CFR 60 defines Frequency-Category 1 and Frequency-Category 2 design basis events and identifies dose consequence limits for these events. In regards to dose limits for Frequency-Category 1 design basis events, 10 CFR 60.2 states:

"Important to safety, with reference to structures, systems, and components, means those engineered features of the repository whose function is:

- (1) To provide reasonable assurance that high-level waste can be received, handled, packaged, stored, emplaced, and retrieved without exceeding the requirements of Part 60.111(a) for Category I design basis events;"

10 CFR 60.111(a) indicates that the geologic repository operations area shall be designed so that until permanent closure has been completed, radiation exposures and levels in unrestricted areas will be maintained within the limits specified in 10 CFR 20. 10 CFR 20.1301(a)(1) limits the dose to individual members of the public to 100 mrem/year TEDE.

In regards to dose limits for Frequency-Category 2 design basis events, 10 CFR 60.2 states:

"Important to safety, with reference to structures, systems, and components, means those engineered features of the repository whose function is:

- (2) To prevent or mitigate Category 2 design basis events that could result in doses equal to or greater than the values specified in Part 60.136 to any individual located on or beyond any point on the boundary of the preclosure controlled area."

10 CFR 60.136 establishes the dose limits for the geologic repository operations area for Category 2 design basis events (5 rem TEDE, along with organ dose limits similar to those in 10 CFR 72.106b for ISFSIs).

In SECY-98-071 (Reference 3), regarding DOE's request for an exemption from the deterministic seismic design requirements of 10 CFR 72.102(f)(1) for an ISFSI that would store TMI-2 spent fuel at INEEL, the NRC staff states:

"With the Part 60 Design basis event rulemaking, NRC adopted a graded approach similar to DOE Standard 1020 for natural hazard characterization and design. The Design basis event rulemaking defined a framework for two SSC design categories for repository surface facilities. For seismic events, the staff has accepted DOE's approach of designing SSCs with failure consequences within the public dose limit of 10 CFR 20.1301(a)(1), 1 mSv (100 mrem), to withstand the 1000-year return period mean ground motion. Meanwhile, SSCs with higher potential accident doses must be designed to withstand the 10,000-year return period mean ground motion."

In the NRC's SER for the 10 CFR 72 license issued for the TMI-2 ISFSI at INEEL (Reference 5, pg. 2-26), the NRC states the following:

"Furthermore, NRC accepted the PSHA method for the design and performance assessment of the proposed high-level waste (HLW) repository at Yucca Mountain (U.S. Department of Energy, 1994c). The NRC has accepted return periods of 1,000 years for Category 1 and 10,000 years for Category 2 DBAs for the PHA estimation for the 100- to 150-year preclosure design life of the proposed HLW repository at Yucca Mountain (U.S. Department of Energy, 1996b)."

There are no dose consequences resulting from a seismic event at the PFSF, since the canisters are shown to retain their integrity and there are no releases of radioactive material. The maximum dose consequence of non-seismic accidents analyzed in the PFSF SAR, postulated canister leakage under hypothetical accident conditions, is approximately 75 mrem TEDE, as discussed above. Since this dose consequence is below the public dose limit of 100 mrem TEDE in 10 CFR 20.1301(a)(1), PFS used the 1,000 year recurrence interval for calculating design basis ground motions. Based on the NRC's risk-informed policy for establishing the DE stated in the above documents, the 1,000 year seismic recurrence interval is appropriate for use at the PFSF since worst-case accident consequences are below the 10 CFR 20.1301(a)(1) public dose limit of 100 mrem.

The 1,000 year recurrence interval is the same as that selected by the DOE for preclosure seismic design of important-to-safety SSCs for Frequency-Category 1 design basis events at the Yucca Mountain high level waste geologic repository in Reference 6, which the NRC staff has accepted. As stated by the DOE in Reference 6, use of a 1,000 year recurrence interval represents a conservative translation of the qualitative frequency description of Frequency-Category 1 design basis events in 10 CFR 60, i.e., "events that are reasonably likely to occur regularly, moderately frequently, or one or more times before permanent closure of the geologic repository operations area." The use of a 1,000 year recurrence interval would be similarly conservative for the PFSF. The license for the PFSF will be for 20 years with the potential for license renewal for another 20 years per 10 CFR 72.42, or up to 40 years, which is a shorter duration than the 150 years considered in Reference 6 (Section 3.1.1) for the Yucca Mountain preclosure facility.

CONCLUSION

Analyses of the effects of the original PFSF site specific design earthquake (0.67g horizontal and 0.69g vertical zero period accelerations) on the HI-STORM and TranStor storage systems have determined that the storage casks remain upright and on the storage pads, with no damage to the canisters and no release of radioactivity. Even if a seismic event of greater magnitude could cause a cask tipover, analyses indicate that the canister confinement barrier would not be

breached and no radioactivity would be released. While there are no radiological consequences resulting from earthquakes, in order to incorporate a conservative margin of safety PFS considered radiological consequences that are associated with other accidents analyzed in the PFSF SAR unrelated to seismic events. Worst case radiological consequences from hypothetical non-seismic accidents are demonstrated to be below the 100 mrem TEDE public dose limit of 10 CFR 20.1301(a)(1). PFS used a 1,000 year recurrence interval for calculating design basis ground motions, which is the recurrence interval adopted by the NRC staff for seismic events which produce dose consequences below 100 mrem TEDE. Given the absence of radiological consequences from any credible seismic event, it is considered that application of the probabilistic risk-informed approach for calculating the seismic hazard that the NRC staff adopted in the Part 60 rulemaking is adequately conservative for the PFSF. Moreover, the expected life span of the PFSF, 20 years with the potential for renewal for another 20 years per 10 CFR 72.42, justifies use of this recurrence frequency.

REFERENCES

1. Geomatrix Consultants, Inc, Deterministic Earthquake Ground Motions Analysis, Private Fuel Storage Facility, Skull Valley, Utah, prepared by Geomatrix Consultants, Inc. and William Lettis & Associates, Inc., GMX#3801.1 (Rev. 0), March 1997.
2. Geomatrix Consultants, Inc., Fault Evaluation Study and Seismic Hazard Assessment, Private Fuel Storage Facility, Skull Valley Utah; Final Report, February 1999.
3. U.S. NRC SECY-98-071, from L. Joseph Callan (EDO) to the Commissioners, "Exemption to 10 CFR 72.102(f)(1) Seismic Design Requirement for Three Mile Island Unit 2 Independent Spent Fuel Storage Installation, dated April 8, 1998.
4. U.S. NRC SECY-98-126, from L. Joseph Callan (EDO) to the Commissioners, "Rulemaking Plan: Geological and Seismological Characteristics for Siting and Design of Dry Cask Independent Spent Fuel Storage Installations, 10 CFR Part 72, dated June 4, 1998.
5. U.S. NRC Safety Evaluation Report of Three Mile Island Unit 2 Independent Spent Fuel Storage Installation Safety Analysis Report, enclosed in U.S. NRC letter dated March 19 1999, from E. W. Brach to W. E. Bergholz, Subject: "Issuance of Materials License SNM-2508 for the Three Mile Island, Unit 2, Independent Spent Fuel Storage Installation."
6. DOE Topical Report YMP/TR-003-NP, Rev. 2, "Preclosure Seismic Design Methodology for a Geologic Repository at Yucca Mountain", August 1997.